iScience

CellPress
OPEN ACCESS

Article

Motor dysfunction in *Drosophila melanogaster* as a biomarker for developmental neurotoxicity

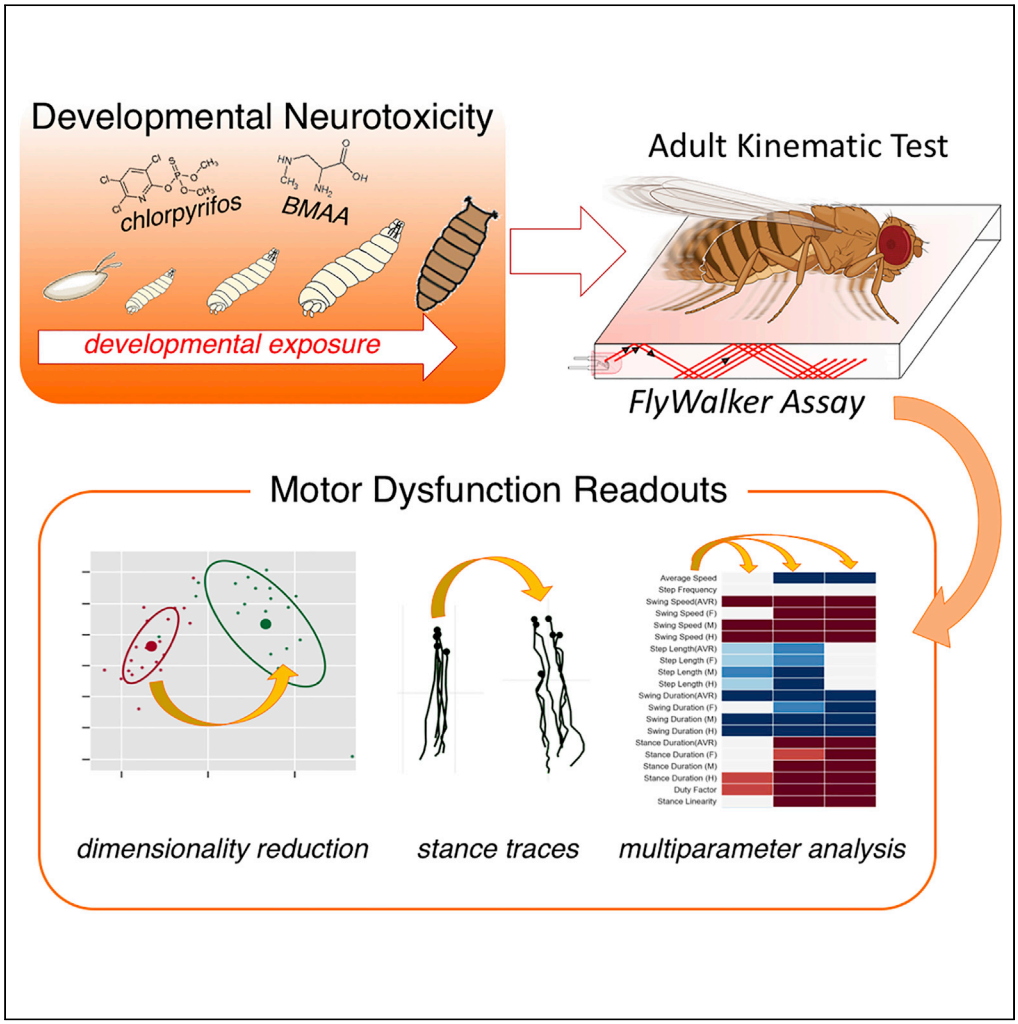

Ana Cabrita, Alexandra M. Medeiros, Telmo Pereira, António Sebastião Rodrigues, Michel Kranendonk, César S. Mendes

michel.kranendonk@nms.unl.pt (M.K.)
cesar.mendes@nms.unl.pt (C.S.M.)

Highlights

Alternatives to mammalian testing are needed to detect developmental neurotoxicity

The pesticide chlorpyrifos causes partial lethality and motor dysfunction

Non-lethal levels of BMAA induce motor dysfunction in a dose-dependent manner

Kinematic profiling of adult *Drosophila* can identify developmental neurotoxicity

Cabrita et al., iScience *25*, 104541
July 15, 2022
https://doi.org/10.1016/j.isci.2022.104541

iScience

CellPress
OPEN ACCESS

Article

Motor dysfunction in *Drosophila melanogaster* as a biomarker for developmental neurotoxicity

Ana Cabrita,[1] Alexandra M. Medeiros,[1] Telmo Pereira,[2] António Sebastião Rodrigues,[3] Michel Kranendonk,[3,*] and César S. Mendes[1,4,*]

SUMMARY

Adequate alternatives to conventional animal testing are needed to study developmental neurotoxicity (DNT). Here, we used kinematic analysis to assess DNT of known (toluene (TOL) and chlorpyrifos (CPS)) and putative (β-N-methylamino-L-alanine (BMAA)) neurotoxic compounds. *Drosophila melanogaster* was exposed to these compounds during development and evaluated for survival and adult kinematic parameters using the FlyWalker system, a kinematics evaluation method. At concentrations that do not induce general toxicity, the solvent DMSO had a significant effect on kinematic parameters. Moreover, while TOL did not significantly induce lethality or kinematic dysfunction, CPS not only induced developmental lethality but also significantly impaired coordination in comparison to DMSO. Interestingly, BMAA, which was not lethal during development, induced motor decay in young adult animals, phenotypically resembling aged flies, an effect later attenuated upon aging. Furthermore, BMAA induced abnormal development of leg motor neuron projections. Our results suggest that our kinematic approach can assess potential DNT of chemical compounds.

INTRODUCTION

Neurotoxicity and developmental neurotoxicity (DNT) are important adverse health effects of environmental contaminants, occupational chemicals, and natural toxins. Moreover, neurotoxicity is one of the most frequently occurring therapeutic drug side effect (Bal-Price et al., 2015b). Exposure to neurotoxicants during development has been recognized to be of particular importance as the developing human brain is inherently more susceptible to damaging agents than is the brain of an adult (Bondy and Campbell, 2005; Rodier, 1995). DNT has been implicated in the etiology of various neuropsychiatric and neurological disorders, including autism spectrum disorder, attention-deficit hyperactive disorder, schizophrenia, Parkinson, and Alzheimer disease (Grandjean and Landrigan, 2014).

Many cellular and molecular processes are known to be crucial for a proper development and function of the central (CNS) and peripheral nervous systems (PNS). However, there are relatively few examples of well-documented pathways for how chemicals may interfere in these processes (Bal-Price and Meek, 2017). The paucity of toxicological data for tens of thousands of chemicals in commercial use and thousands of new chemicals produced each year has called the attention during the last decade, for development of sensitive and rapid assays to screen for their neurotoxic propensity, particular for DNT (Smirnova et al., 2014).

The main reason for the lack of data lies in the current guidelines (OECD TG 426 and US EPA 712-C-98-239; OECD, 2007; US EPA, 1998) largely based on *in vivo* experiments, which are costly, time consuming, and unsuitable for testing large numbers of chemicals (Bal-Price et al., 2012). Therefore, there is a need for adequate alternatives to conventional animal testing for neurotoxicity and DNT (Bal-Price et al., 2012). Hence, efforts are being directed toward the development of alternative models, utilizing either mammalian cells in culture or non-mammalian model systems, with the inclusion of new testing strategies to facilitate transition to more mechanistically based approaches (Xie et al., 2020). Such approaches can unveil mechanistic cues that can assist in optimizing sensitive and practical assay endpoints for pathway-specific screening and the determination of predictive key events, which can be used as biomarkers for specific neurotoxic outcomes (Bal-Price and Meek, 2017). Models such as zebrafish, *Caenorhabditis elegans*, and *Drosophila melanogaster* are increasingly recognized for their suitability to test a larger number of

[1]iNOVA4Health, NOVA Medical School|Faculdade de Ciências Médicas, NMS|FCM, Universidade Nova de Lisboa, Lisboa, Portugal

[2]NOVA Medical School| Faculdade de Ciências Médicas, NMS|FCM, Universidade Nova de Lisboa, Lisboa, Portugal

[3]ToxOmics, NOVA Medical School|Faculdade de Ciências Médicas, NMS|FCM, Universidade Nova de Lisboa, Lisboa, Portugal

[4]Lead contact

*Correspondence: michel.kranendonk@nms.unl.pt (M.K.), cesar.mendes@nms.unl.pt (C.S.M.)

https://doi.org/10.1016/j.isci.2022.104541

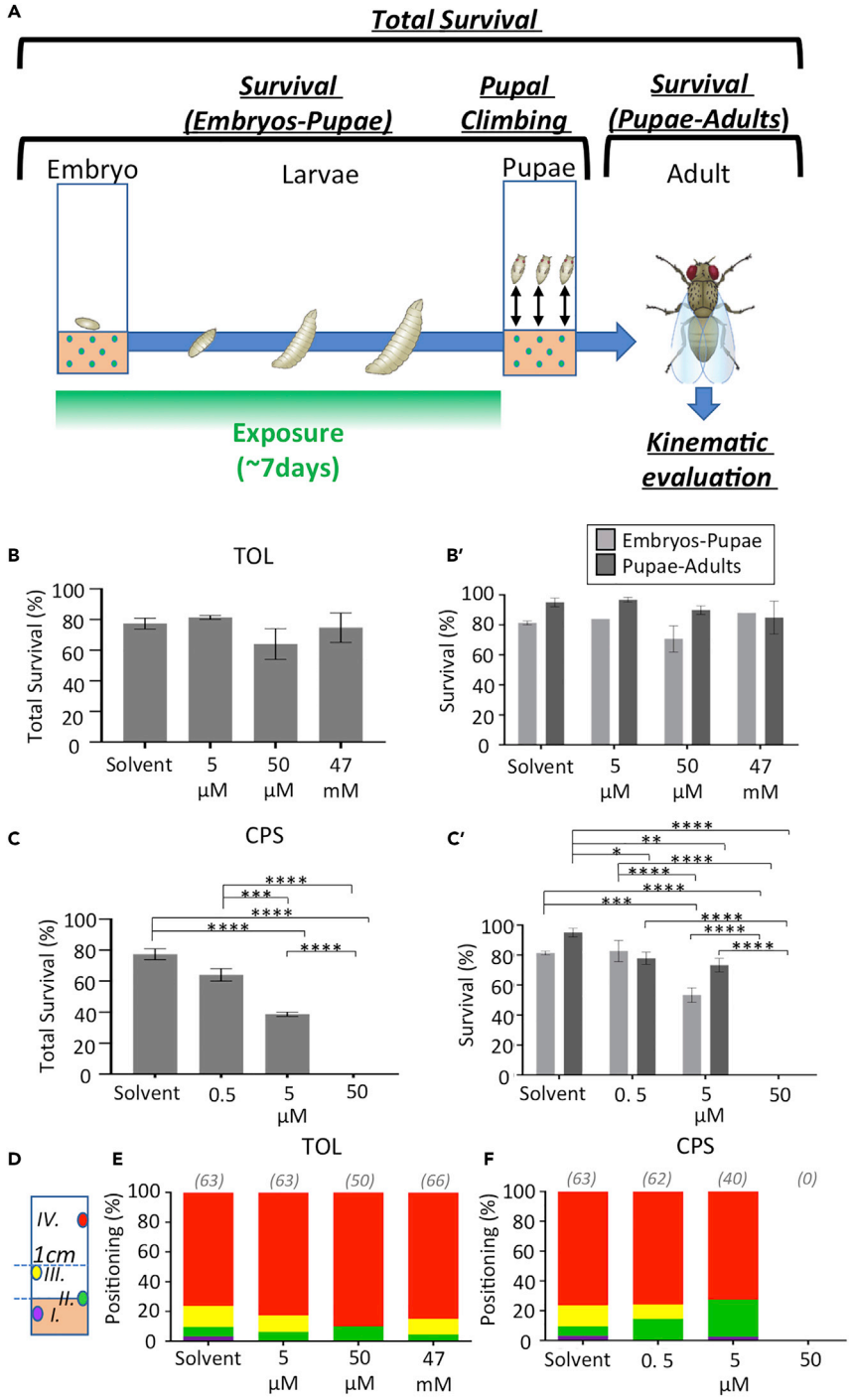

Figure 1. Measurements of pupal and adult survival of *Drosophila melanogaster* developing in the presence of the neurotoxic agents TOL and CPS

(A) Schematic of the procedure and metrics used in this study. Embryos are placed in tainted or untainted food (control). Several parameters were quantified in this study (in *italic*), see main text for details.

(B and C) Survival of adult animals, which were exposed during development to increasing concentrations of (B) TOL (0; 5 µM; 50 µM or 47 mM; n = 75 for each condition) and (C) CPS (0; 0.5; five or; 50 µM) compared to solvent (DMSO; n = 75 for each condition). *p < 0.05; **p < 0.01; ***p < 0.001. (B′, C′) Partial survival scores. Light gray represents embryo to pupae survival, and dark gray represents pupae to adult survival.

Figure 1. *Continued*
(D–F) Pupal distance. (D) Climbing scoring scheme: Pupal positions were divided into four groups: I. (purple) inside the food; II. (green) slightly above the food; III. (yellow) up to 1 cm from the food; and IV. (red) occupying the area above 1 cm. (D) Pupal distance represented as a percentage stacked bar graph for increasing concentrations of (E) TOL and (F) CPS compared to solvent (DMSO). Number of animals tested (n) is indicated in the figure. See STAR Methods for details.

candidate compounds, in addition to acquire "mode of action" type of information regarding neurotoxicity, and neurological disorders and diseases (Peterson et al., 2008). The fruit fly *D. melanogaster* has got particular attention in the modern regimen of neurotoxicological testing due to similarities of their neurological and developmental pathways with those of vertebrates (Rand, 2010), emphasizing its unique attributes for assaying neurodevelopment and behavior (Affleck and Walker, 2019; Rand et al., 2019). Recent investigations have propagated several powerful assay methods with *Drosophila* in developmental and behavioral toxicology (Rand, 2010). However, most studies rely on parameters that poorly reflect neuronal defects or decay. In these studies, several parameters are tested in an attempt to find parameters indicative of more general toxicity such as mortality, female-male ratio, DNA damage (Cox et al., 2016), climbing assay, alteration in acetylcholinesterase activity, and other enzymes (Dinter et al., 2016; Rand et al., 2014). Despite their usefulness, climbing assays only provide low resolution in distinguishing different experimental conditions, i.e., just a one-dimensional perspective of a complex and multidimensional phenomenon such as multi-jointed walking, highly dependent on a properly developed and fine-tuned nervous system. Coordinated walking in vertebrates and multi-legged invertebrates such as *D. melanogaster* requires a complex neural network coupled to sensory feedback (Dickinson et al., 2000). Perturbation of such neural networks in humans has been indicated as the source of several neurological disorders, in which exposure to neurotoxic chemicals was implicated (Grandjean and Landrigan, 2014).

The combination of increasingly sophisticated optical systems with computer algorithms has allowed to track movement of multi-segmented body parts with high spatiotemporal resolution and extract a multitude of quantifiable data that accurately describe walking performance (Berman et al., 2014; Günel et al., 2019; Kain et al., 2013; Mathis et al., 2018; Mendes et al., 2013; Pereira et al., 2019; Uhlmann et al., 2017; Wu et al., 2019). Such tools have identified the effects on the motor system of internal and external manipulations such as increased body load or lack of a particular neurotransmitter, among others (Enriquez et al., 2015; Howard et al., 2019; Mendes et al., 2014; Schretter et al., 2018).

In the current report, we describe the use of *D. melanogaster* as a model to study the DNT of two known neurotoxic agents standardly applied in testing, namely the solvent toluene (TOL) and the pesticide chlorpyrifos (CPS) (Aschner et al., 2017), in addition to testing the putative neurotoxic agent β-N-methylamino-L-alanine (BMAA) (Weiss and Choi, 1988). For this, we combined classical metrics such as animal survival with a sensitive and detailed kinematic assay that accurately and quantitatively reports the status of the motor system (Mendes et al., 2013), using it as indicator of DNT.

RESULTS

Effect of DMSO, TOL, and CPS on developmental survival

Two known neurotoxins, applied as standards in neurotoxicity screenings, were used to study their effect on the development of *D. melanogaster,* by transferring fertilized eggs into food containing defined concentrations of these compounds (Figure 1A). We chose the aromatic hydrocarbon TOL, widely used as a solvent, in addition to its usage as a recreational drug (Filley et al., 2004), and the commonly used organophosphate pesticide CPS.

Drosophila's development from an egg to adult takes approximately 11 days at 25°C, comprising a stationary embryonic stage, lasting 22 h. (Ashburner, 1989), followed by three larval stages, in which activity consists of mostly food consumption with a duration of four days. Subsequently, third-instar larvae crawl away from their food source and start a molting process outside the food source, undergoing a metamorphosis process lasting approximately 3 days (Denlinger and Zdarek, 1994; Heredia et al., 2021; Markow et al., 2009; Powsner, 1935). The development of any multicellular organism depends on the rigorous execution of a specific developmental and genetic program. As this developmental process is highly sensitive to chemical insults, we measured initially three developmental features: i) survival from egg to adult, ii) egg to pupae, and iii) pupae to adult (Figure 1A), an approach described previously (Khatun et al., 2018; Nazir et al., 2001; Zhou et al., 2010a). Owing to poor aqueous solubility, both TOL and CPS were diluted in aqueous DMSO,

which although is used widely as solvent in experimental biology and a preferred cryoprotectant, can *per se* induce developmental toxicity (Gurtovenko and Anwar, 2007; Nazir et al., 2003; Uysal et al., 2015) and neurotoxicity (Awan et al., 2020; Bakar et al., 2012). Control experiments were performed, testing several food concentrations of DMSO at pupal and adult stages, to determine a concentration that would allow to predilute TOL and CPS, without interference of this solvent (Figure S1; see STAR Methods). A concentration of 140 mM DMSO in fly food induced a reduced number of enclosed animals (hatching from the pupal case), consequence of a reduced pupal to adult transition (Figure S1B). However, lower concentrations of DMSO displayed little or no effect on survival, and a 70 mM aqueous solution of DMSO was subsequently used as solvent for TOL and CPS (Figure S1B). Exposure of developing *Drosophila* to increasing concentrations of CPS during development showed a dose-dependent lethality with concentrations as low as 5 μM showing an approximately 50% reduction in the number of animals reaching adulthood (Figure 1C). Additional drop in survival (approximately 22%) was found during the pupa to adult transition (Figure 1C'), indicating the detrimental effect of CPS even after animals ceased to be exposed to the tainted food. A 50 μM concentration of CPS induced complete lethality with no animals reaching the pupal stage (Figure 1C').

In *Drosophila*, the feeding larval stage is followed by a wandering phase where larvae exit the food to find an appropriate pupation site (Denlinger and Zdarek, 1994). The pupation traveling distance can be influenced by genetic traits and external factors such as moisture and environmental cues (Beltramí et al., 2010; Johnson and Carder, 2012; Narasimha et al., 2015; Sokolowski and Bauer, 1989). This distance has been used in different paradigms, including exposure of the developing larva to toxic compounds, as a marker for fitness of the neuromuscular system to drive the crawling larva to a safe location for metamorphosis (Johnson and Carder, 2012; Joshi and Mueller, 1993; Khatun et al., 2018; Sood et al., 2019). Accordingly, we measured the pupation distance by recording the position of pupa relative to the food level in four categories: I. within the food, II. slightly above the food line, III. up to 1 cm from the food, and IV. above 1 cm mark (Figure 1D).

Exposure to TOL during development did not influence the pupal positioning even at higher concentrations with most (>76%) of wondering larvae pupating at a position higher than 1 cm from the food (Figure 1E and Table S1). Moreover, no statistically significant difference in pupal positioning was detected between the solvent and tested TOL concentrations (Table S1). These results are consistent with a lack of lethality observed previously (Figure 1B), further suggesting that TOL does not impair the larval neuromuscular system while exposed to the tainted food in these conditions. Similarly, increasing concentrations of CPS did not significantly change the percentage of pupae located beyond the 1 cm mark (76 $\pm$ 10% for control condition vs 76 $\pm$ 7% and 73 $\pm$ 1%, for 0.5 and 5 μM, respectively; Figure 1F and Table S1). Moreover, there was an increase, albeit non-significant, in the number of pupae present at the food interface, simultaneously matched by a decrease of pupa above the food line but below the one cm mark (Figure 1F and Table S1). Although statistical analysis did not show a difference between these groups, these data suggest that CPS can affect the ability of wandering larva to emerge from the food, in order to pupate. Overall, these results show that two known neurotoxic agents—TOL and CPS—can have distinct effects on the ability of *Drosophila* to survive development. While CPS induced lethality at relatively low concentrations, TOL was unable to influence the survival rate even at a high dose of food exposure.

Effect of DMSO, TOL, and CPS on adult kinematics

While surviving adult animals that developed in the presence of TOL and CPS did not show clear anatomical defects (data not shown), we tested if there were any detrimental effects of these known neurotoxins on coordination in their walking conduct (Figure 2). For this purpose, a standardized pipeline was followed from sample preparation to kinematic output generation (Figure S2 and STAR Methods). Walking behavior of multi-segmented organisms such as *Drosophila* displays a highly reproducible and stereotyped pattern aimed to move the animal in an energy-efficient and stable fashion (Mendes et al., 2013; Ramdya et al., 2017; Strauss and Heisenberg, 1990; Szczecinski et al., 2018; Wosnitza et al., 2013). However, disruption of the motor neuronal circuit has direct consequences on gait properties of walking animals. For example, inactivation of serotonergic neurons in the ventral nerve cord of *Drosophila* (the analog of the mammalian spinal cord) has a significant effect on gait properties (Howard et al., 2019). We thus considered that exposure to neurotoxins may not lead to lethality during development but nevertheless could affect the proper development and function of the motor nervous system. To test this hypothesis, we analyzed the kinematic behavior of untethered adult flies, which during development were exposed to food containing non-lethal

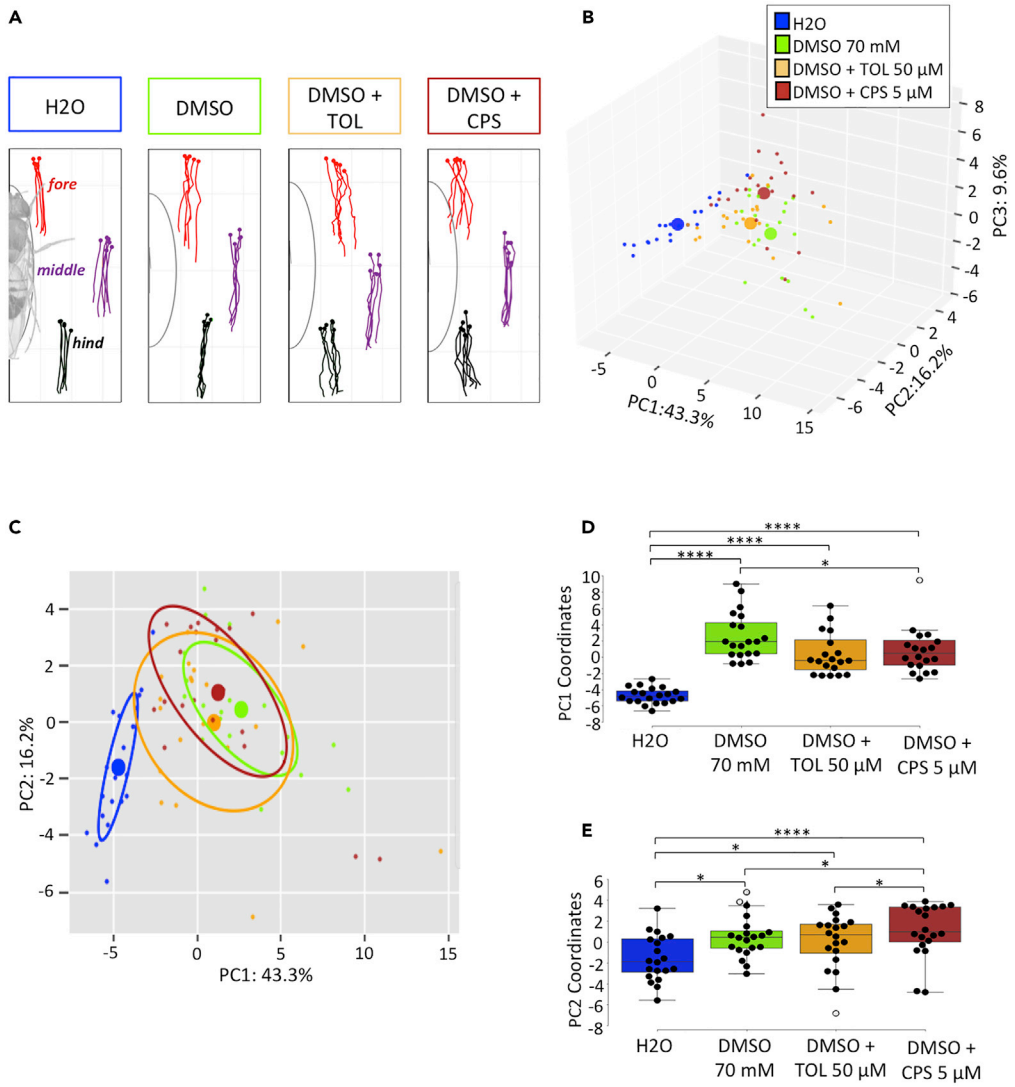

Figure 2. Kinematic parameters of adult animals exposed during development to water, 70 mM DMSO (solvent), DMSO plus 50 µM TOL, and DMSO plus 5 µM CPS

One-week-old animals were exposed during development to water, 70 mM DMSO (solvent), DMSO plus 50 µM TOL, and DMSO plus 5 µM CPS and kinematics features were recorded and analyzed using the FlyWalker system (n = 20 for each condition).

(A) Representative stance traces (normalized to body-length represented by the oval shape), which marks the tarsal contacts relative to the body axis during stance phases. See (Mendes et al., 2013) for details. (B–C) PCA of all kinematic parameters.

(B) Tridimensional representation of three-component PCA analysis. Each individual small dot represents one video while larger dots represent the average point (n = 20 for each condition). Contribution of each component is indicated in each axis.

(C) 2D representation with ellipses delimiting 50% of variance of the data.

(D and E) Comparison of each PC coordinate. *p < 0.05, **p < 0.01. ***p < 0.001. (D) PC1 coordinates. (E) PC2 coordinates. See STAR Methods for details.

levels of TOL (50 µM) or CPS (5 µM) using the FlyWalker system. This approach allows the extraction of a large set of kinematic parameters with a high spatiotemporal resolution (Mendes et al., 2013) (Figures 2, S3, and S4).

We compared the kinematic performance of adult animals developing in the presence of water, 70 mM of the solvent DMSO, the solvent plus 50 µM TOL, and the solvent plus 5 µM CPS (Figures 2, S3, and S4). When

compared to water, animals developing in the presence of the aqueous DMSO alone or in combination with 50 μM TOL or 5 μM CPS displayed stance phases with inconsistent leg positioning relative to the body axis, including during touch-down and swing-onset (Figure 2A).

By further analyzing the kinematic features of our experimental conditions, we found an effect on a large number of parameters compared to water (Figure S3A). Moreover, by comparing the performance of 70 mM DMSO supplemented with 50 μM TOL, we found a shift in six of the 39 parameters analyzed, with some alterations targeting the front and middle hemi-segments (Figure S3B). In contrast, we found that 5 μM CPS induced kinematic alterations on 15 parameters (Figure S3B and Video S1), most notably on step frequency, step length, and stance straightness, which measures the consistency of the stance phase (or power stroke), indicating that CPS promotes an aggravated uncoordinated walking behavior compared to its solvent (Figure S4).

We subsequently subjected all the kinematic parameters to a three-order principal component analysis (PCA) generating a three-dimensional representation (Figures 2B–2E). We chose this dimensionality reduction method due to its general acceptance, ease of implementation, in addition for its ability to reduce redundancy in an unsupervised manner and not biased by class-structures (for review see (Bishop, 2006; Postma et al., 2009). 3D and 2D scatterplots display the spatial distribution of each experimental condition among the most representative components (Figures 2B and 2C, respectively). PC1, representing 43.3% variance of the dataset, allowed the discrimination of exposure between water vs. DMSO and DMSO vs. DMSO plus 5 μM CPS (Figures 2C and 2D). Moreover, PC2, representing 16.2% variation variance, also allowed the differentiation of animals exposed to DMSO alone vs. supplemented with CPS (Figures 2C and 2E), further indicating a kinematic effect induced by the exposure to CPS during development. These data also show that while TOL can induce a shift in a few kinematic parameters, it does occupy the same behavioral space compared to the solvent DMSO, which could have masked any possible DNT effect (Coecke et al., 2016). As a negative control, we also tested the effect of glycerol, a common polar organic solvent with very low toxicity (Figure S5). Although some kinematic parameters were affected, PCA analysis shows that animals exposed to 68 mM glycerol during development did not occupy a different behavioral space compared to water.

Altogether, our results support that animals, although surviving exposure to specific levels of neurotoxic agents during development, may display motor dysfunction, highlighting the presence of neuronal defects. Our data also indicate that DMSO may mask DNT effects in *Drosophila*, which can hamper an adequate assessment of test compounds. This is an important issue for *in vitro* toxicological studies in general regarding solvents that can *per se* induce a biological effect (Coecke et al., 2016). Nevertheless, our data analysis highlighted the ability of our FlyWalker approach to quantitatively identify CPS as capable to induce kinematic dysfunction and thus developmental neurotoxicity.

Effect of BMAA on developmental survival

Subsequently, we evaluated the effect of BMAA on the development of *Drosophila*. The non-proteinogenic amino acid BMAA has been suggested to induce neurotoxic effects and has been implicated in the etiology of amyotrophic lateral sclerosis (ALS) (Banack et al., 2015; Jonasson et al., 2010; Lobner et al., 2007; Muñoz-Sáez et al., 2015; Murch et al., 2004; Pablo et al., 2009; Proctor et al., 2019; Roy-Lachapelle et al., 2017; Weiss et al., 1989). Former studies of BMAA in *Drosophila* showed that BMAA severely reduced life span, climbing capabilities, and memory (Zhou et al., 2009, 2010b). Interestingly, our data show that exposure to increasing food concentrations of BMAA did not affect the survival of developing *Drosophila*, with similar number of animals reaching adulthood and pupal stages compared to control animals (solvent, i.e., water) (Figures 3A and 3B). Still, BMAA induced a shift in pupal positioning from positions below or at the food level, a strong indication for larval neuromuscular system impairment, to positions located further away from the food source (Figure 3C and Table S2), suggesting a potential repellent, or escaping effect of BMAA on wandering third-instar larvae.

We also tested the climbing capabilities of animals developing under the presence of growing concentrations of BMAA (Figure 3D). Flies have the innate behavior to move against gravity (termed negative geotaxis), and a reduced climbing performance is indicative of motor dysfunction (Dinter et al., 2016; Ganetzky and Flanagan, 1978). Moreover, continuous exposure of adult flies to 2–8 mM BMAA induced climbing defects (Zhou et al., 2009, 2010b). Using this assay, we found that only the highest concentration of

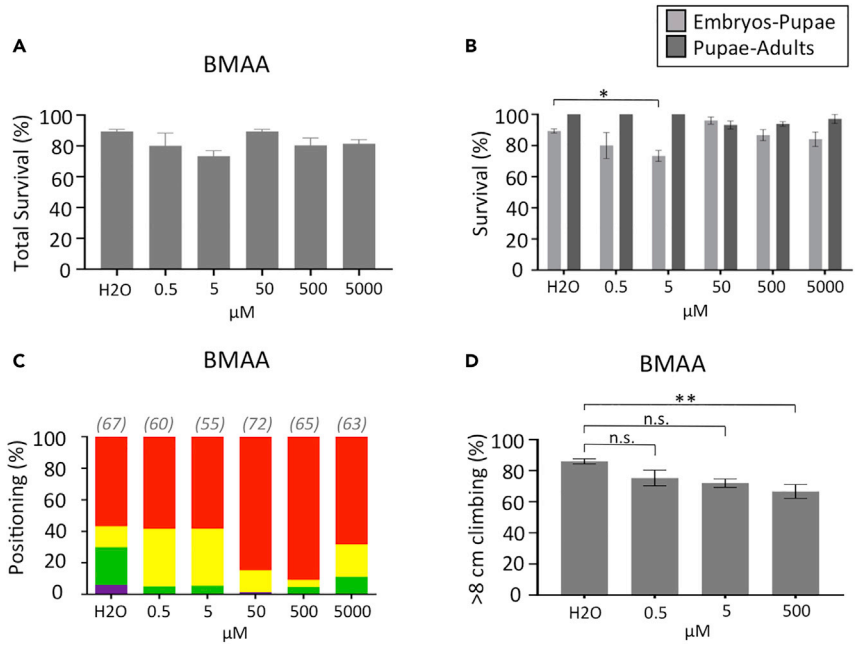

Figure 3. Pupal and adult survival of *Drosophila melanogaster* developing in the presence of the BMAA

(A) Survival of adult animals developing in increasing concentrations of BMAA (0; 0.5; 5 or 500 µM) compared to solvent (water; n = 75 for each condition).

(B) Partial survival scores. Light gray represents embryo to pupae survival, and dark gray represents pupae to adult survival.

(C) Pupal distance. Pupal positions were divided into four groups: I. (purple) inside the food; II. (green) slightly above the food; III. (yellow) up to 1 cm from the food; and IV. (red) occupying the area above 1 cm. Number of animals tested (n) is indicated in the figure. Results represented as a percentage stacked bar graph for increasing concentrations BMAA compared to solvent (water).

(D) Climbing performance of 1-week old animals developing in increasing concentrations of BMAA (0; 0.5; 5 or 500 µM) compared to solvent (water; n = 50 for each condition). For each condition, groups of 10 animals were tested for the ability to climb the 8 cm mark after 10 s **p < 0.01. n.s., not significant. See STAR Methods for details.

500 µM induced a statistical difference compared to the solvent (Figure 3D). Thus, using this metric, developmental neurotoxicity induced by BMAA is only measurable at higher concentrations.

Effect of BMAA on adult kinematics

We next tested if developing *Drosophila* exposed to increasing food concentrations of BMAA displayed kinematic dysfunction, using the FlyWalker system, including at lower concentrations where the climbing assay failed to identify a significant effect (Figure 3D). We found that 1-week-old adult *Drosophila* displayed a dose-depended motor dysfunction when exposed to increasing concentrations of BMAA during development (Figures 4 and S6 and Video S2). All parameter classes were altered and stance phases display an increasingly inconsistent leg positioning relative to the body axis, including during touch-down and swing-onset (Figures 4A and 4B). The PCA analysis indicated a 44.5% variance of data by PC1 (Figures 4C and 4D), and 2D visualization shows that increasing concentrations of BMAA corresponded to a stronger effect (i.e., dose-response), relative to the control condition (Figure 4D). While PC1 analysis quantitatively shows a dose-response effect, PC2 representing 17.1% variance only discriminated intermediate concentrations of BMAA compared to control groups (Figure 4F), indicating the capture of the most relevant variation in motor function by PC1. Similarly, individual analysis of gait parameters confirmed the aforementioned trend, with several parameters showing increasing divergence from control conditions with increased concentrations of BMAA (Figure S6).

Time effect of BMAA-induced motor dysfunction

We subsequently verified the effect of aging and the reversibility of BMAA-induced motor dysfunction. For this, we evaluated kinematic performance using the FlyWalker system of 3-week-old flies maintained on

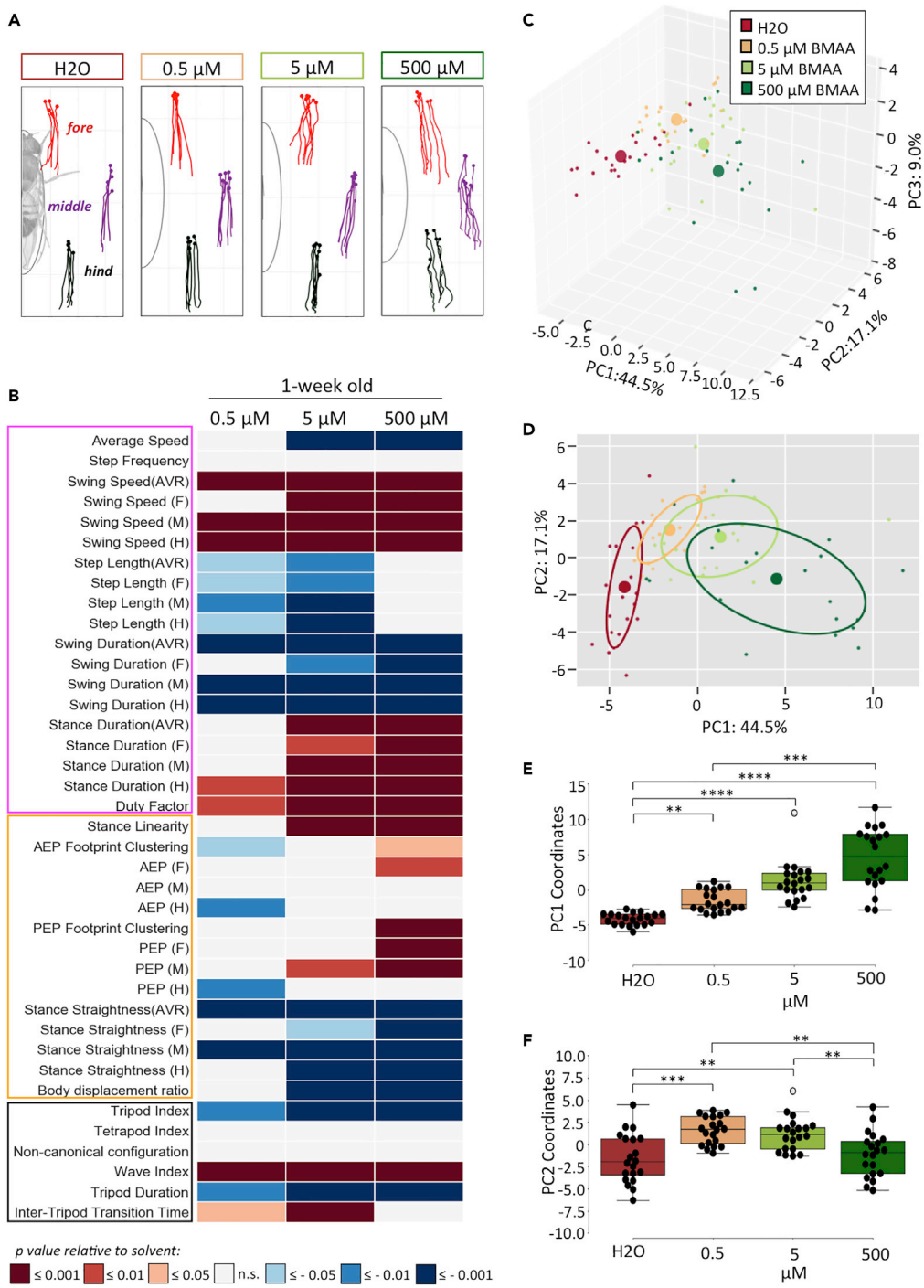

Figure 4. Kinematic parameters of one-week adult animals exposed to increasing concentrations of BMAA during development

Exposure levels were 0, 0.5, 5, or 500 µM of BMAA. Kinematic features were recorded and analyzed using the FlyWalker system (n = 20 for each condition).

(A) Representative stance traces, which mark the tarsal contacts relative to the body axis during stance phases, (see (Mendes et al., 2013) for details).

(B) Heatmap of kinematic parameters. Features are distinguished by "Step" (pink box), "Spatial" (yellow box), and "Gait" (black box), parameters. For each parameter, values are matched to animals exposed to solvent (water) and p values are

Figure 4. *Continued*
represented by a color code with red and blue shades indicate a decrease or increase relative to control, respectively. White indicates no variation.
(C–F) PCA of all kinematic parameters. (C) Tridimensional representation of three-component PCA analysis. Each individual small dot represents one video while larger dots represent the average point (n = 20 for each condition). Contribution of each component is indicated in each axis; (D) 2D representation with ellipses delimiting 50% of variance of the data. (E–F) Comparison of each PC coordinate. **p < 0.01, ***p < 0.001, ****p < 0.0001. (E) PC1 coordinates. (F) PC2 coordinates. See STAR Methods for details.

normal, untainted food, but exposed during their development to increasing concentrations of BMAA. Because *Drosophila* have a life expectancy of ~60 days with a 50% survival rate of 40 days (Ashburner, 1989), we first tested if aging *per se* could affect kinematic features. Interestingly, we found that 3-week-old flies display alterations in many parameters, including spatial parameters, consistent with age-related movement uncoordination (Figures S7 and S8). Similar to 1-week-old animals, we found a dose-dependent effect of BMAA on kinematic features of this older age group (Figures 5 and S9). Higher concentrations of BMAA induced a more significant uncoordinated stance profile (Figure 5A) and larger differences when compared to control conditions (Figure 5B). However, two noteworthy aspects should be highlighted. Firstly, compared to control animals, the impact of BMAA exposure in 3-week-old animals appears to be reduced when compared to 1-week-old animals. For example, exposure to 0.5 μM of BMAA during development affects many of the kinematic parameters in 1-week-old animals (Figure 4A), while in 3-week-old animals only one parameter showed a significant difference to control conditions (Figures 5 and S9). Secondly, while in 1-week-old animals a seemingly linear dose dependence in response on kinematic effects can be observed (Figures 4E and S6), this is not the case for 3-week-old animals in which lower and intermediate concentrations of BMAA occupy a similar pattern to control conditions in a PCA (Figures 5C and 5D). These results suggest an adaptation of the neuromuscular system regarding the detrimental effect of BMAA during development. Nevertheless, at higher concentrations of BMAA (500 μM), this compensatory effect was less pronounced, visible through the heatmap pattern and PCA quantification (Figures 5B, 5E, and 5F), suggesting a threshold concentration for which the neurodevelopmental impairment no longer can be compensated and becomes permanent.

Subsequently, we tested the hypothesis that the motor dysfunction induced by BMAA, particularly at higher concentrations, could include a time-dependent neurodegenerative component beyond the initial neurodevelopmental effect. To test this hypothesis, we compared the behavioral 3-dimensional PCA of 1- and 3-week-old animals exposed to increasing concentrations of BMAA during development (Figure 6). Interestingly, we found that aging did not exacerbate the differences between the control condition and flies reared in the presence of BMAA, even at the maximum concentration of 500 μM. These results support the model that BMAA interferes with the proper development of the neuromuscular system leading to an uncoordinated phenotype.

Effect of BMAA on motor neuron targeting

We found that exposure to BMAA during development induces motor impairments during adulthood (Figures 4, 5, 6, and S6–S9). Neurodevelopmental dysfunction of motor neurons has been shown to cause motor impairments with dendritic or axonal mistargeting, causing abnormal execution of motor commands (Enriquez et al., 2015). We hypothesized that the neuromuscular system is targeted by BMAA, resulting in an uncoordinated walking pattern. We thus tested if the motor defects induced by the developmental exposure to BMAA could be caused by a defect of the muscular fibers or a neurodevelopmental defect of the motor neurons.

We first tested if defects in muscular fibers were responsible for the motor phenotype observed. For this, we used a *Drosophila* strain that expresses a GFP fusion protein of tropomyosin 1 (Buszczak et al., 2007), an integral component of actin filaments within muscle fibers (Lehman et al., 2009; Schachat et al., 1985; Wang et al., 1990), generating a muscle pattern that can be visualized by confocal microscopy (Figure S10). Animals exposed to 500 μM BMAA did not demonstrate any defect in their tropomyosin 1-GFP muscle pattern, both in general pattern and periodicity (Figures S10A–S10C), indicating that muscular dysfunction is not the cause of mobility coordination defects caused by BMAA.

We next questioned if development of motor neurons could be influenced by BMAA. To test this hypothesis, we genetically labeled the neuromuscular junction (NMJ) of a single motor neuron enervating the tibia

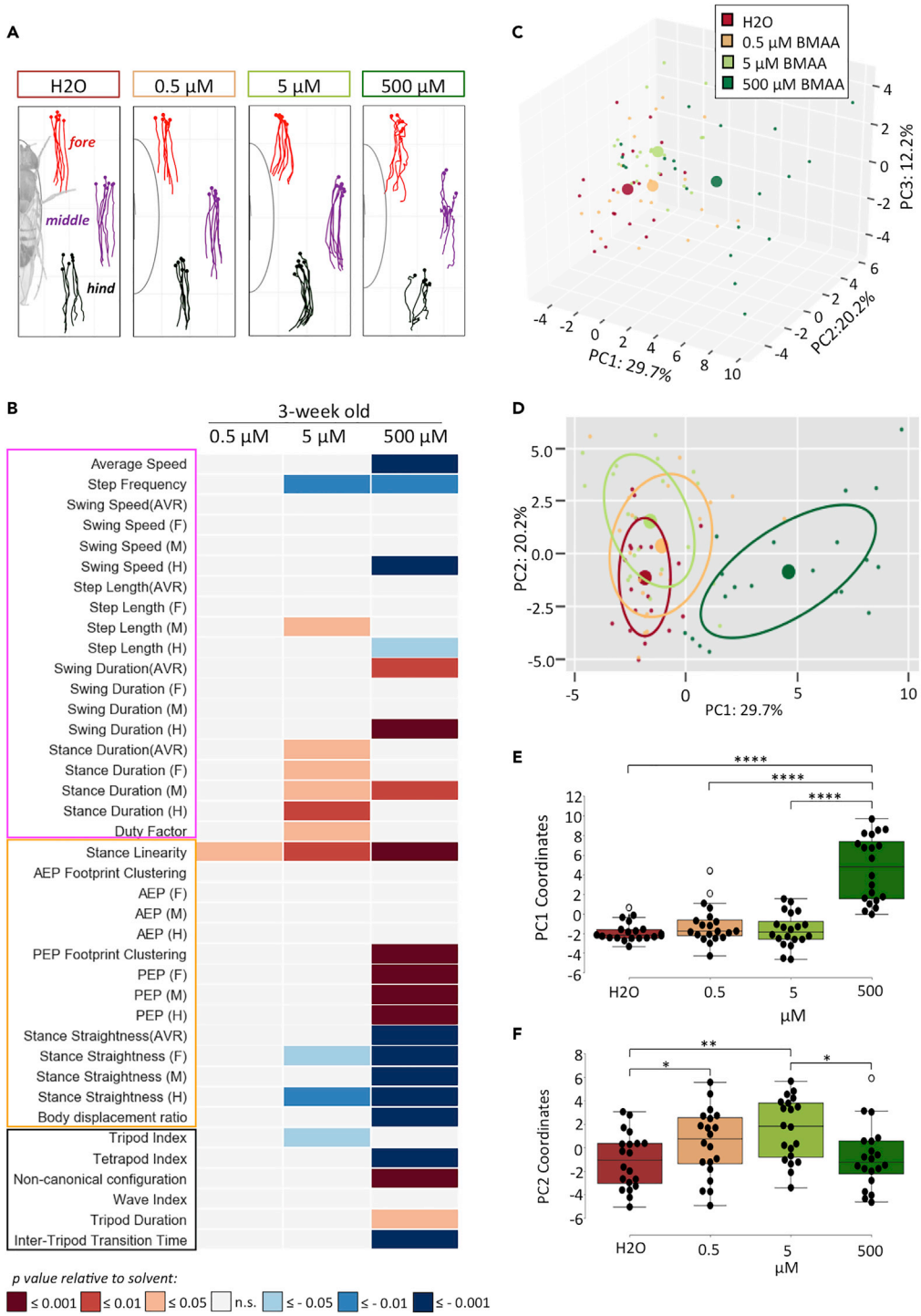

Figure 5. Kinematic parameters of 3-week adult animals exposed to increasing concentrations of BMAA during development

Exposure levels were 0, 0.5, 5, or 500 µM of BMAA. Kinematics features were recorded and analyzed using the FlyWalker system (n = 20 for each condition).

(A and B) Representative stance traces, which mark the tarsal contacts relative to the body axis during stance phases (see Mendes et al. (2013) for details) (B) Heatmap of kinematic parameters. Features are distinguished by "Step" (pink box), "Spatial" (yellow box), and "Gait" (black box), parameters. For each parameter, values were matched to animals exposed

Figure 5. *Continued*
to solvent (water) and p values are represented by a color code with red and blue shades indicate a decrease or increase relative to control, respectively. White indicates no variation.
(C–F) PCA of all kinematic parameters. (C) Tridimensional representation of three-component PCA analysis. Each individual small dot represents one video while larger dots represent the average point (n = 20 for each condition). Contribution of each component is indicated in each axis. (D) 2D representation with ellipses delimiting 50% of variance of the data. (E-F) Comparison of each PC coordinate. *p < 0.05, **p < 0.01, ****p < 0.0001. (E) PC1 coordinates. (F) PC2 coordinates. See STAR Methods for details.

depressor muscle (tidm) within the proximal femur (Azevedo et al., 2020; Soler et al., 2004) (Figure 7A). This was obtained by expressing the Rab3-YFP fusion protein that marks presynaptic sites (Zhang et al., 2007), driven by a motor neuron-specific promoter (Azevedo et al., 2020). Three-week-old control (solvent exposed) animals displayed a normal NMJ pattern, very similar to the one previously reported (Azevedo et al., 2020) (Figure 7B). Strikingly, we found that exposure to 500 μM of BMAA during development induced an altered NMJ pattern, with projections located more dorsally, closer to the center of the femur, while targeting the same tidm muscle (Figures 7C–7F and Video S3). Moreover, BMAA-exposed animals displayed a more linear axonal profile compared to control animals, which showed a more twisted appearance (Figures 7E′ and 7G and Video S3). It should be noted that other metrics, such as the number of branches and the most distal position, remain unchanged (Figures S10D and S10E and data not shown). These results indicate that although animals developing in the presence of BMAA display an altered neuronal pattern, no signs of neurodegeneration were visible, consistent with the kinematic results observed previously (Figure 6). As such, BMAA exposure during development can induce an altered motor neuron profile, which can ultimately be responsible for an impaired walking performance.

DISCUSSION

Here, we present data on the use of a *D. melanogaster* model for DNT studies, using a kinematic assay that accurately and quantitatively reports the status of the motor system.

Our results indicate that this test strategy can identify changes in the neuromuscular system that strongly matches the predicted neurotoxic effect of CPS, affecting several motor parameters without affecting survival during development (Figures 1, 2, S3, and S4). Noteworthy, while we also observed a significant kinematic dysfunction in flies exposed to DMSO (Figures 2 and S3), we could still resolve the kinematic effect of the additional presence of CPS further validating the usefulness of our approach.

Moreover, we found that the putative neurotoxic agent BMAA induces strong motor defects in a dose-dependent fashion in adult animals exposed to this compound during development, possibly by inducing motor neuron mistargeting, without inducing lethality (Figures 3, 4, 5, 6, 7, and S6–S10). Importantly, using the climbing assay, we failed to identify motor dysfunction in adult animals exposed to 0.5 and 5 μM BMAA during development (Figure 3D), strongly suggesting a higher sensitivity of the FlyWalker approach.

Exposure to neurotoxic agents can adversely interfere with the function and development of the nervous system in humans (Grandjean and Landrigan, 2006). Several chemical substances have been shown to induce DNT, given the susceptibility of the developing brain (Aschner et al., 2017). Nevertheless, neurotoxicity has also been reported in adult exposure, including environmental and in occupational settings. Known neurotoxic agents include mercury, lead, methylmercury, polychlorinated biphenyls, arsenic, and toluene (Grandjean and Landrigan, 2006, 2014). The assessment of neurotoxicity is usually carried out using OECD test guidelines and those of other national regulatory agencies (US EPA, guidelines), based on animal models. These models assess changes in neuroanatomical, neurophysiological, neurochemical, and neurobehavioral parameters (Makris et al., 2009). However, there is a paucity of data on DNT. Of the 350,000 chemicals in use globally (Wang et al., 2020), DNT data are only available for approximately 110–140 compounds (Sachana et al., 2021). Current data requirements for *in vivo* DNT testing are considered insufficient to adequately screen and characterize compounds potentially hazardous for the human developing brain (Bal-Price et al., 2015a). Therefore, a pressing need exists for developing alternative methods that can more rapidly and cost effectively support the identification and characterization of chemicals with DNT potential. Alternative DNT testing methods have been proposed, including human *in vitro* models, non-mammalian 3Rs models, and *in silico* approaches (Bal-Price and Fritsche, 2018).

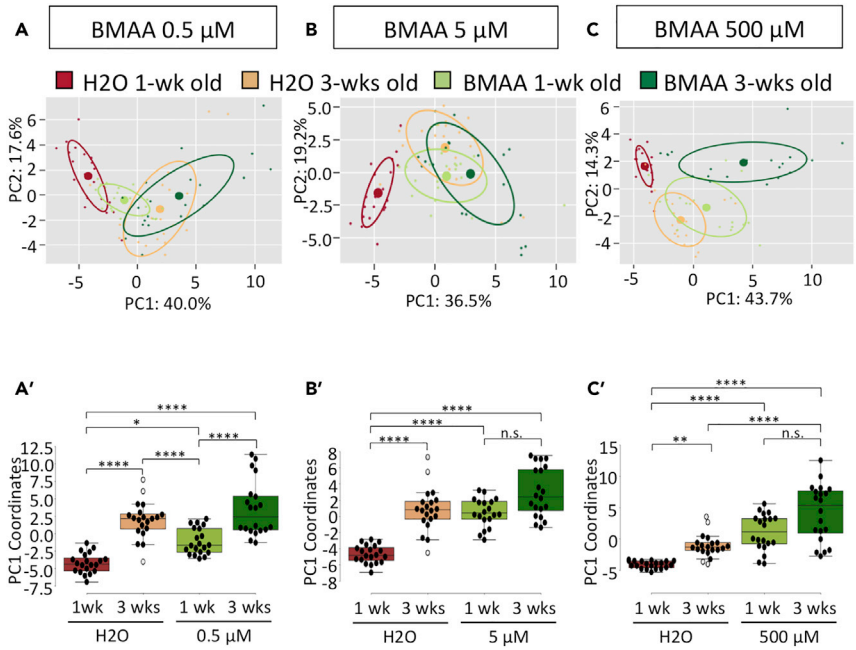

Figure 6. Time effect on motor dysfunction induced by BMAA neurotoxicity

(A–C) Animals were exposed to solvent (water); 0.5, 5, or 500 µM of BMAA during development and maintained for one and three weeks before being tested for kinematic features using the FlyWalker system (n = 20 for each condition). Data are represented as a 2D representation of a three-component PCA. Each individual small dot represents one video while larger dots represent the average point, with ellipses delimiting 50% of variance of the data (n = 20 for each condition). Contribution of each component is indicated in each axis (A'-C') Comparison of PC1 coordinates. *p < 0.05, **p < 0.01, ***p < 0.001, n.s., not significant.

Two of the compounds tested here, TOL and CPS, present strong evidence for DNT effects in humans and are listed as a reference compound for validation of alternative test methods to indicate DNT potential (Aschner et al., 2017).

Our data indicate that exposure of developing *Drosophila* to increasing concentrations of TOL did not significantly induce lethality or pupal positioning at any developmental stage, while the same type of exposure to CPS showed a dose-dependent lethality (Figure 1). The lack of overt lethality to TOL could be due to several factors. Although TOL is a volatile compound, the chosen exposure route was via food; therefore, uptake was essentially through ingestion, although contact exposure and volatilization cannot be excluded. Alternatively, metabolization of TOL to toxic metabolites may occur less efficiently during developmental stages. Moreover, TOL did not show significant motor dysfunction, using the PCA as a criterion to identify DNT (Figure 2), albeit the large body of evidence describing TOL as a neurotoxic compound (Echeverria et al., 1989; Filley et al., 2004; Hersh, 1989; Zeng et al., 2014). Among the reasons for this, detection failure could be the concentration of TOL used in our assay (50 µM), a masking by the solvent DMSO (Coecke et al., 2016), or as with the lethality assay, using ingestion as the delivery method. Previous studies using *Drosophila* have identified motor dysfunction after exposure to volatile compounds including TOL. Tatum-Gibbs et al. exposed flies for 4 h to an atmosphere containing 175 to 1400 ppm TOL, and observed a narcotic effect. However, motor activity returned to pre-exposure levels when the vapor was removed from the air, indicating a transient effect (Tatum-Gibbs et al., 2015). Although acute toxicity studies have been performed in *Drosophila* (Adebambo et al., 2020; Bushnell et al., 2017; Tatum-Gibbs et al., 2015), to the best of our knowledge, no DNT studies with TOL were described so far, for this model. Neurotoxicity has been identified by inhalation studies in humans and animals as a critical endpoint (Cruz et al., 2014). However, limited neurotoxicity studies by the oral route are available (Ameno et al., 1989). Data suggest that TOL generally does not elicit developmental effects except at doses that are significantly higher than those causing other systemic perturbations (EPA., 2005; Tyle et al., 2003).

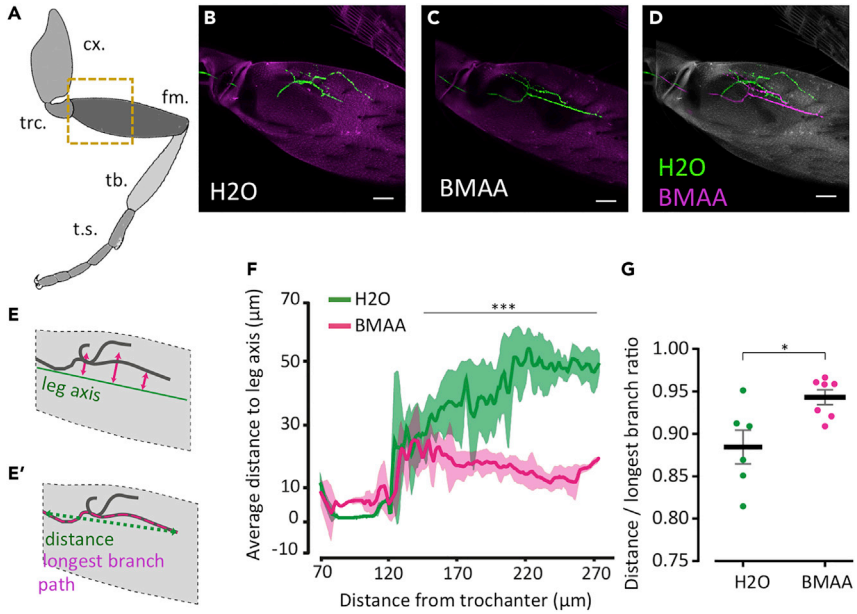

Figure 7. Long-term effect on motor neuron morphology by exposure to BMAA during development

Animals were exposed to solvent (water) and 500 µM of BMAA during development and maintained on untainted food for three weeks before being examined. Genotype: R22A08-LexA/+; lexOp-Rab3:YFP/+.

(A) Schematic representation of the fly leg. cx., coxa; trc., trochanter; fm., femur; tb., tibia; t.s., tarsal segments. Dashed square represents the scanned region in B–D.

(B and C) Representative projections of a single motor neuron in the proximal femur (green) and cuticle autofluorescence (pink) in control animals (B) and exposed to 500 µM of BMAA during development (C). Bar, 30 µm.

(D) Overlapped projections of the aligned images shown in B (green) and C (pink). Cuticle autofluorescence (white). Bar, 30 µm.

(E and F) Schematic of the quantification presented in (F). The average distance to leg axis was calculated by measuring the distance between a line along the center of the femur to the average YFP signal perpendicular to the proximal-distal axis. (E') Schematic of the quantification presented in (G). The distance to longest-branch ratio was measured by identifying the longest branch from the trochanter-femur joint and calculating the ratio between the distance of the longest branch and its straight-line path. See STAR Methods for details. (F) Average distance to leg axis along the proximal-distal axis. Average values for animals developing in water (green, n = 6) or BMAA (pink, n = 7) are represented with shadowed areas representing SD. Statistical analysis between 150 and 270 µm using Mann-Whitney non-parametric test, ****$p < 0.0001$).

(G) Distance to longest branch ratio was calculated for animals developing in water (green, n = 6) or BMAA (pink, n = 7). *$p < 0.01$.

CPS is a chlorinated organophosphorus ester widely used as an insecticide in agricultural settings. CPS acts by inhibiting the enzyme acetylcholinesterase (AChE), thus preventing the degradation of the neurotransmitter acetylcholine (ACh) within synaptic clefts, both at neuromuscular or neuroglandular junctions. This leads to ACh accumulation and cholinergic hyperstimulation (Casida, 2017). CPS is highly lipophilic and is readily absorbed through the skin and lungs. CPS is also quickly absorbed through the placenta into fetal tissues and it has been implicated in learning and behavioral effects, including developmental delays related to cognition and motor function, attention-deficit hyperactivity disorder, autism spectrum disorder (ASD), and tremors (Bai et al., 2014; Gray and Lawler, 2011; Rauh et al., 2011, 2012, 2015). CPS toxicity has been evaluated in several model systems, including rats, zebrafish, and *C. elegans*, with some replicating the neurotoxic effects observed in humans (Silva, 2020). In our system, CPS displayed an impact on 15 motor parameters, most notably step and spatial parameters, suggesting that both motor and pre-motor centers at the level of the ventral nerve cord (the equivalent of the vertebrate spinal cord) are targeted leading to an uncoordinated walking behavior. Overall, the CPS dataset supports the sensitivity and detailed motor information obtained with the FlyWalker approach on this known neurotoxic agent, largely coinciding with its known mode of action, with additional mechanistic clues.

While DMSO was used as a non-toxic solvent to prepare working solutions of CPS, the significant kinematic dysfunction observed was unexpected since there was no observed lethality at the concentration

used. DMSO is an aprotic solvent that can solubilize a wide variety of otherwise poorly soluble polar and nonpolar molecules for which there are no alternative solvents ((Santos et al., 2003); OECD Guidance Document on Good *In Vitro* Method Practices (GIVIMP)). At commonly used concentrations, as was the case in our study, 70 mM corresponding to 0.5% (v/v), DMSO is not cytotoxic, and indeed has several pharmacological uses, such as an anti-inflammatory and reactive oxygen species scavenger (Santos et al., 2003), and is routinely used as a cryoprotectant in autologous bone marrow and organ transplantation. DMSO is considered a relatively safe solvent in doses up to 50 mg per day (Hanslick et al., 2009). Nevertheless, DMSO readily crosses the blood–brain barrier, and has been reported to be neurotoxic. The quantitative nature of the FlyWalker system allows us to quantitatively compare different experimental conditions, delineating the simultaneous effect of two neurotoxic compounds, further validating our approach.

Particular attention was paid to BMAA since from the three tested compounds, it was the less studied and has been implicated in several neurodegenerative conditions (Kurland, 1988). BMAA is a natural non-proteinaceous amino acid produced by cyanobacteria (Cox et al., 2005), diatoms (Jiang et al., 2014) and dinoflagellates (Lage et al., 2014). Neurotoxicity of BMAA has been reported in various studies (Cox et al., 2005; Spencer et al., 1987). Particular interest in BMAA arose from the association with endemic neurodegenerative diseases, such as Parkinson-dementia complex and ALS, in the indigenous people of Guam (Kurland, 1988). Intense research efforts have identified various possible mechanisms of neurotoxicity, including misincorporation into cellular proteins, which may lead to adverse effects (Dunlop et al., 2013; Dunlop and Guillemin, 2019). BMAA is excitotoxic against neurons via glutamate receptors (Weiss and Choi, 1988), and also displays suppression of cell cycle progression of non-neuronal NIH3T3 cells (Okamoto et al., 2018).

None of the BMAA concentrations tested affected the survival rates (Figure 3), eclosion timing, or external morphology (not shown). However, increasing concentrations of BMAA rendered walking increasingly uncoordinated (Figures 4 and S6, and Video S2), further suggesting a higher sensitivity of the developing neuronal system to toxic insults. This correlation between dosage and phenotype was attenuated in 3-week-old animals, suggesting adaptation of the neuromuscular system to long-term motor constrains, leading to a shift in the walking behavior. Such adaptation has been described previously after long-term weight bearing or injury (Isakov et al., 2016; Mendes et al., 2014), underscoring a potential form of motor plasticity.

Our data indicate that BMAA exposure during development does not trigger acute adult neurodegeneration, instead promotes motor dysfunction phenotypically resembling aging. This conclusion is based on two observations: First, non-exposed aged animals displayed a coordination phenotype resembling young animals exposed to higher BMAA exposures (3-weeks-old control animals resemble 1-week-old animals exposed to BMAA during development, see Figures 6B′ and 6C′). Second, although the motor neuron analysis displayed an altered axonal pattern in animals raised on BMAA (Figure 7), these do not show any metrics consistent with degeneration (Figures 7 and S10). The observed effects of BMAA on motor neuron targeting suggest that the misincorporation of BMAA into proteins, critical for the proper wiring of neuronal circuits, such as transcriptional regulators or cell adhesion receptors, may alter synaptic terminal differentiation phenotypes, ultimately leading to motor and, potentially, cognitive defects (Enriquez et al., 2015; Skarlatou et al., 2020; Venkatasubramanian et al., 2019).

It should be noted that our study focused on the effects of neurotoxic compounds during development, as adults were fed non-tainted food, and the reported neurodegenerative effects are probably due to a continuous exposure to BMAA (Kurland, 1988). Although it was out of the scope of this study, it would be interesting to test the long-term effects of BMAA in motor neurons degeneration and kinematic activity, or if alternatively, neurons become more susceptible to additional insults.

According to OECD, DNT has been regarded as an area in need of time- and cost-effective *in vitro* testing methods for predictive outcomes as well for regulatory decisions (Fritsche et al., 2017). Accordingly, several alternative *in vitro* and *in silico* DNT models have been proposed, as well as non-rodent animal models, most notably, the climbing assay in flies. Here, we provide evidence for the use of the FlyWalker as an additional method to identify DNT due to its vast kinematic profile and sensitivity. In addition, our kinematic assay was also able to identify aging-associated alterations in kinematic parameters in 3-week-old flies,

suggesting its additional usefulness studying aging processes. In this regard, exposure to neurotoxic agents may accelerate the dysfunction observed in aged individuals. Furthermore, the cost associated with the methodology described here is much lower when compared with rodent *in vivo* assays.

Finally, the rich dataset generated by the FlyWalker software requires a proper *post hoc* analysis method, such as PCA, which provides a simple and powerful approach to identify global kinematic changes caused by test compounds (Figure S2 and see STAR Methods). Nevertheless, other methodologies for dimensionality reduction could be implemented for specific objectives (Anowar et al., 2021; Bishop, 2006; Postma et al., 2009).

Overall, our results highlight the potential of detailed motor surveillance tools in simpler and more approachable model systems for the identification of neurotoxicity, with the potential to provide important cues. These cues can be subsequently explored in finding predictive key events of pathways leading to DNT, which may serve as sensitive and practical read-outs in the evaluation of DNT of chemicals. By using the extensive genetic toolkit of *Drosophila* currently available, one may further explore such cues to obtain additional insights on the mode of action (MoA) of neurotoxins. One could compare kinematic parameter patterns of known neurotoxins i.e., with identified MoAs, with patterns obtained from yet to be identified neurotoxins, for the identification of type(s) of MoA(s) in their potential DNT. This could assist in the confirmation of key events and/or obtaining additional ones, useful for evaluation of chemical DNT.

Limitations of the study

Exposure assessment to test compounds was not performed, thus we do not know the actual exposure to the agents in individual flies. Nevertheless, it is not feasible to calculate the individual intake of each fly during larval stages. A further limitation, as exemplified with TOL, is the difficulty assessing DNT of volatile compounds in the current setup. The application of the FlyWalker for the determination of DNT was only demonstrated by testing few compounds; testing additional compounds (both known and unknown neurotoxins) is necessary to further validate this approach.

STAR★METHODS

Detailed methods are provided in the online version of this paper and include the following:

- KEY RESOURCES TABLE
  - Lead contact
  - Materials availability
- EXPERIMENTAL MODEL AND SUBJECT DETAILS
- METHOD DETAILS
  - Generation of transgenic lines
  - Embryo collection
  - Food preparation
  - Survival and pupal climbing positioning
  - Climbing assay
  - Kinematic analysis
  - Leg dissection and microscopy
- QUANTIFICATION AND STATISTICAL ANALYSIS
  - FlyWalker data
  - PCA
  - Microscopy data
  - Graphs and statistical analyses

SUPPLEMENTAL INFORMATION

Supplemental information can be found online at https://doi.org/10.1016/j.isci.2022.104541.

ACKNOWLEDGMENTS

We thank Matthew Scott and Jun Zhang for the Rab3:YFP plasmid, John Tuthill for suggesting the R22A08 driver, Mendes lab, Rita Teodoro and her lab for comments and suggestions during the execution of this project, Allan Mancoo for assistance in the design of the PCA script, Daniela Pereira and Edgar Gomes for

comments on the manuscript. We thank the scientific and technical assistance from the Microscopy and Fly facilities. We also thank CONGENTO: consortium for genetically tractable organisms and the Bloomington Drosophila Stock Center for fly stocks. This work was supported by H2020 Marie Skłodowska-Curie Actions (H2020-MSCA-IF-2016, #752891, GEMiNI to CSM), Fundação para a Ciência e a Tecnologia (FCT) (PTDC/BIA-COM/0151/2020, iNOVA4Health (UIDB/04462/2020 and UIDP/04462/2020), and LS4FUTURE (LA/P/0087/2020) to CSM). AM was supported by a doctoral fellowship from FCT (PD/BD/128445/2017). ASR and MK were partially supported by grant UID/BIM/0009/2020 for the Research Center for Toxicogenomics and Human Health - (ToxOmics) from FCT, Portugal.

AUTHOR CONTRIBUTIONS

ASR, MK, and CSM contributed to conception and design of the study. AC and CSM performed the experiments. AC, AM, and TP analyzed the raw data. AC, ASR, MK, and CSM wrote the manuscript. All authors contributed to manuscript revision, read, and approved the submitted version.

DECLARATION OF INTERESTS

The authors declare no competing interests.

Received: July 11, 2021
Revised: October 30, 2021
Accepted: June 2, 2022
Published: July 15, 2022

REFERENCES

Adebambo, T.H., Fox, D.T., and Otitoloju, A.A. (2020). Toxicological study and genetic basis of BTEX susceptibility in Drosophila melanogaster. Front. Genet. *11*, 1275.

Affleck, J.G., and Walker, V.K. (2019). Drosophila as a model for developmental toxicology: using and extending the drosophotoxicology model. Methods Mol. Biol. *1965*, 139–153. https://doi.org/10.1007/978-1-4939-9182-2_10.

Ameno, K., Fuke, C., Ameno, S., Kiriu, T., Sogo, K., and Ijiri, I. (1989). A fatal case of oral ingestion of toluene. Forensic Sci. Int. *41*, 255–260. https://doi.org/10.1016/0379-0738(89)90218-1.

Anowar, F., Sadaoui, S., and Selim, B. (2021). Conceptual and empirical comparison of dimensionality reduction algorithms (PCA, KPCA, LDA, MDS, SVD, LLE, ISOMAP, LE, ICA, t-SNE). Computer Science Review *40*, 100378. https://doi.org/10.1016/j.cosrev.2021.100378.

Aschner, M., Ceccatelli, S., Daneshian, M., Fritsche, E., Hasiwa, N., Hartung, T., Hogberg, H.T., Leist, M., Li, A., Mundi, W.R., et al. (2017). Reference compounds for alternative test methods to indicate developmental neurotoxicity (DNT) potential of chemicals: example lists and criteria for their selection and use. ALTEX *34*, 49–74. https://doi.org/10.14573/altex.1604201.

Ashburner, M. (1989). Drosophila: A Laboratory Manual (Cold Spring Harbor Laboratory).

Awan, M., Buriak, I., Fleck, R., Fuller, B., Goltsev, A., Kerby, J., Lowdell, M., Mericka, P., Petrenko, A., Petrenko, Y., et al. (2020). Dimethyl sulfoxide: a central player since the dawn of cryobiology, is efficacy balanced by toxicity? Regenerative medicine *15*, 1463–1491. https://doi.org/10.2217/rme-2019-0145.

Azevedo, A.W., Dickinson, E.S., Gurung, P., Venkatasubramanian, L., Mann, R.S., and Tuthill, J.C. (2020). A size principle for recruitment of Drosophila leg motor neurons. Elife *9*, e56754. https://doi.org/10.7554/eLife.56754.

Bai, W.D., Ye, X.M., Zhang, M.Y., Zhu, H.Y., Xi, W.J., Huang, X., Zhao, J., Gu, B., Zheng, G.X., Yang, A.G., and Jia, L.T. (2014). MiR-200c suppresses TGF-β signaling and counteracts trastuzumab resistance and metastasis by targeting ZNF217 and ZEB1 in breast cancer. Int. J. Cancer *135*, 1356–1368. https://doi.org/10.1002/ijc.28782.

Bakar, B., Kose, E.A., Sonal, S., Alhan, A., Kilinc, K., and Keskil, I.S. (2012). Evaluation of the neurotoxicity of DMSO infused into the carotid artery of rat. Injury *43*, 315–322. https://doi.org/10.1016/j.injury.2011.08.021.

Bal-Price, A., Crofton, K.M., Leist, M., Allen, S., Arand, M., Buetler, T., Delrue, N., FitzGerald, R.E., Hartung, T., Heinonen, T., et al. (2015a). International STakeholder NETwork (ISTNET): creating a developmental neurotoxicity (DNT) testing road map for regulatory purposes. Arch. Toxicol. *89*, 269–287. https://doi.org/10.1007/s00204-015-1464-2.

Bal-Price, A., Crofton, K.M., Sachana, M., Shafer, T.J., Behl, M., Forsby, A., Hargreaves, A., Landesmann, B., Lein, P.J., Louisse, J., et al. (2015b). Putative adverse outcome pathways relevant to neurotoxicity. Crit. Rev. Toxicol. *45*, 83–91. https://doi.org/10.3109/10408444.2014.981331.

Bal-Price, A., and Fritsche, E. (2018). Editorial: developmental neurotoxicity. Toxicol. Appl. Pharmacol. *354*, 1–2. https://doi.org/10.1016/j.taap.2018.07.016.

Bal-Price, A., and Meek, M.E.B. (2017). Adverse outcome pathways: application to enhance mechanistic understanding of neurotoxicity. Pharmacology & therapeutics *179*, 84–95. https://doi.org/10.1016/j.pharmthera.2017.05.006.

Bal-Price, A.K., Coecke, S., Costa, L., Crofton, K.M., Fritsche, E., Goldberg, A., Grandjean, P., Lein, P.J., Li, A., Lucchini, R., et al. (2012). Advancing the science of developmental neurotoxicity (DNT): testing for better safety evaluation. ALTEX *29*, 202–215. https://doi.org/10.14573/altex.2012.2.202.

Banack, S.A., Caller, T., Henegan, P., Haney, J., Murby, A., Metcalf, J.S., Powell, J., Cox, P.A., and Stommel, E. (2015). Detection of cyanotoxins, β-N-methylamino-L-alanine and microcystins, from a lake surrounded by cases of amyotrophic lateral sclerosis. Toxins *7*, 322–336. https://doi.org/10.3390/toxins7020322.

Beltramí, M., Medina-Muñoz, M.C., Arce, D., and Godoy-Herrera, R. (2010). Drosophila pupation behavior in the wild. Evol. Ecol. *24*, 347–358. https://doi.org/10.1007/s10682-009-9310-8.

Berman, G.J., Choi, D.M., Bialek, W., and Shaevitz, J.W. (2014). Mapping the stereotyped behaviour of freely moving fruit flies. J. R. Soc. Interface/the Royal Society *11*. https://doi.org/10.1098/rsif.2014.0672.

Bishop, C.M. (2006). Pattern Recognition and Machine Learning (Springer).

Bondy, S.C., and Campbell, A. (2005). Developmental neurotoxicology. J. Neurosci. Res. *81*, 605–612. https://doi.org/10.1002/jnr.20589.

Bushnell, P.J., Ward, W.O., Morozova, T.V., Oshiro, W.M., Lin, M.T., Judson, R.S., Hester, S.D., McKee, J.M., and Higuchi, M. (2017). Editor's highlight: genetic targets of acute toluene inhalation in Drosophila melanogaster. Toxicol. Sci. : an official journal of the Society of

Toxicology *156*, 230–239. https://doi.org/10.1093/toxsci/kfw243.

Buszczak, M., Paterno, S., Lighthouse, D., Bachman, J., Planck, J., Owen, S., Skora, A.D., Nystul, T.G., Ohlstein, B., Allen, A., et al. (2007). The carnegie protein trap library: a versatile tool for Drosophila developmental studies. Genetics *175*, 1505–1531. https://doi.org/10.1534/genetics.106.065961.

Casida, J.E. (2017). Organophosphorus xenobiotic toxicology. Annu. Rev. Pharmacol. Toxicol. *57*, 309–327. https://doi.org/10.1146/annurev-pharmtox-010716-104926.

Coecke, S., Bernasconi, C., Bowe, G., Bostroem, A.C., Burton, J., Cole, T., Fortaner, S., Gouliarmou, V., Gray, A., Griesinger, C., et al. (2016). Practical aspects of designing and conducting validation studies involving multi-study trials. Adv. Exp. Med. Biol. *856*, 133–163. https://doi.org/10.1007/978-3-319-33826-2_5.

Cox, P.A., Banack, S.A., Murch, S.J., Rasmussen, U., Tien, G., Bidigare, R.R., Metcalf, J.S., Morrison, L.F., Codd, G.A., and Bergman, B. (2005). Diverse taxa of cyanobacteria produce beta-N-methylamino-L-alanine, a neurotoxic amino acid. Proc. Natl. Acad. Sci. U. S. A. *102*, 5074–5078. https://doi.org/10.1073/pnas.0501526102.

Cox, P.A., Davis, D.A., Mash, D.C., Metcalf, J.S., and Banack, S.A. (2016). Dietary exposure to an environmental toxin triggers neurofibrillary tangles and amyloid deposits in the brain. Proceedings. Biological sciences *283*. https://doi.org/10.1098/rspb.2015.2397.

Cruz, S.L., Rivera-García, M.T., and Woodward, J.J. (2014). Review of toluene action: clinical evidence, animal studies and molecular targets. J. Drug Alcohol Res. *3*, 235840. https://doi.org/10.4303/jdar/235840.

Denlinger, D.L., and Zdarek, J. (1994). Metamorphosis behavior of flies. Annu. Rev. Entomol. *39*, 243–266. https://doi.org/10.1146/annurev.en.39.010194.001331.

Dickinson, M.H., Farley, C.T., Full, R.J., Koehl, M.A., Kram, R., and Lehman, S. (2000). How animals move: an integrative view. Science *288*, 100–106.

Dinter, E., Saridaki, T., Nippold, M., Plum, S., Diederichs, L., Komnig, D., Fensky, L., May, C., Marcus, K., Voigt, A., et al. (2016). Rab7 induces clearance of α-synuclein aggregates. J. Neurochem. *138*, 758–774. https://doi.org/10.1111/jnc.13712.

Dunlop, R.A., Cox, P.A., Banack, S.A., and Rodgers, K.J. (2013). The non-protein amino acid BMAA is misincorporated into human proteins in place of L-serine causing protein misfolding and aggregation. PLoS One *8*, e75376. https://doi.org/10.1371/journal.pone.0075376.

Dunlop, R.A., and Guillemin, G.J. (2019). The cyanotoxin and non-protein amino acid β-methylamino-L-alanine (L-BMAA) in the food chain: incorporation into proteins and its impact on human health. Neurotox. Res. *36*, 602–611. https://doi.org/10.1007/s12640-019-00089-9.

Echeverria, D., Fine, L., Langolf, G., Schork, A., and Sampaio, C. (1989). Acute neurobehavioural effects of toluene. Br. J. Ind. Med. *46*, 483–495. https://doi.org/10.1136/oem.46.7.483.

Enriquez, J., Venkatasubramanian, L., Baek, M., Peterson, M., Aghayeva, U., and Mann, R.S. (2015). Specification of individual adult motor neuron morphologies by combinatorial transcription factor codes. Neuron. https://doi.org/10.1016/j.neuron.2015.04.011.

EPA, U. (2005). Toxicological Review of Toluene in Support of Summary Information on the Integrated Risk Information System (IRIS) (US Environmental Protection Agency Washington^ eDC DC).

Filley, C.M., Halliday, W., and Kleinschmidt-DeMasters, B.K. (2004). The effects of toluene on the central nervous system. Journal of neuropathology and experimental neurology *63*, 1–12. https://doi.org/10.1093/jnen/63.1.1.

Fritsche, E., Crofton, K.M., Hernandez, A.F., Hougaard Bennekou, S., Leist, M., Bal-Price, A., Reaves, E., Wilks, M.F., Terron, A., Solecki, R., et al. (2017). OECD/EFSA workshop on developmental neurotoxicity (DNT): the use of non-animal test methods for regulatory purposes. ALTEX *34*, 311–315. https://doi.org/10.14573/altex.1701171.

Ganetzky, B., and Flanagan, J.R. (1978). On the relationship between senescence and age-related changes in two wild-type strains of Drosophila melanogaster. Exp. Gerontol. *13*, 189–196.

Grandjean, P., and Landrigan, P.J. (2006). Developmental neurotoxicity of industrial chemicals. Lancet (London, England) *368*, 2167–2178. https://doi.org/10.1016/s0140-6736(06)69665-7.

Grandjean, P., and Landrigan, P.J. (2014). Neurobehavioural effects of developmental toxicity. Lancet Neurol. *13*, 330–338. https://doi.org/10.1016/s1474-4422(13)70278-3.

Gray, K., and Lawler, C.P. (2011). Strength in numbers: three separate studies link in utero organophosphate pesticide exposure and cognitive development. Environmental health perspectives *119*, A328–A329. https://doi.org/10.1289/ehp.1104137.

Günel, S., Rhodin, H., Morales, D., Campagnolo, J., Ramdya, P., and Fua, P. (2019). DeepFly3D, a deep learning-based approach for 3D limb and appendage tracking in tethered, adult Drosophila. Elife *8*. https://doi.org/10.7554/eLife.48571.

Gurtovenko, A.A., and Anwar, J. (2007). Modulating the structure and properties of cell membranes: the molecular mechanism of action of dimethyl sulfoxide. The journal of physical chemistry. B *111*, 10453–10460. https://doi.org/10.1021/jp073113e.

Hanslick, J.L., Lau, K., Noguchi, K.K., Olney, J.W., Zorumski, C.F., Mennerick, S., and Farber, N.B. (2009). Dimethyl sulfoxide (DMSO) produces widespread apoptosis in the developing central nervous system. Neurobiol. Dis. *34*, 1–10. https://doi.org/10.1016/j.nbd.2008.11.006.

Heredia, F., Volonté, Y., Pereirinha, J., Fernandez-Acosta, M., Casimiro, A.P., Belém, C.G., Viegas, F., Tanaka, K., Menezes, J., Arana, M., et al. (2021). The steroid-hormone ecdysone coordinates parallel pupariation neuromotor and morphogenetic subprograms via epidermis-to-neuron Dilp8-Lgr3 signal induction. Nat. Commun. *12*, 3328. https://doi.org/10.1038/s41467-021-23218-5.

Hersh, J.H. (1989). Toluene embryopathy: two new cases. J. Med. Genet. *26*, 333–337. https://doi.org/10.1136/jmg.26.5.333.

Howard, C.E., Chen, C.L., Tabachnik, T., Hormigo, R., Ramdya, P., and Mann, R.S. (2019). Serotonergic modulation of walking in Drosophila. Curr. Biol. *29*, 4218–4230. e4218. https://doi.org/10.1016/j.cub.2019.10.042.

Isakov, A., Buchanan, S.M., Sullivan, B., Ramachandran, A., Chapman, J.K., Lu, E.S., Mahadevan, L., and de Bivort, B. (2016). Recovery of locomotion after injury in Drosophila melanogaster depends on proprioception. J. Exp. Biol. *219*, 1760–1771. https://doi.org/10.1242/jeb.133652.

Jiang, L., Eriksson, J., Lage, S., Jonasson, S., Shams, S., Mehine, M., Ilag, L.L., and Rasmussen, U. (2014). Diatoms: a novel source for the neurotoxin BMAA in aquatic environments. PLoS One *9*, e84578. https://doi.org/10.1371/journal.pone.0084578.

Johnson, W.A., and Carder, J.W. (2012). Drosophila nociceptors mediate larval aversion to dry surface environments utilizing both the painless TRP channel and the DEG/ENaC subunit, PPK1. PLoS One *7*, e32878. https://doi.org/10.1371/journal.pone.0032878.

Jonasson, S., Eriksson, J., Berntzon, L., Spácil, Z., Ilag, L.L., Ronnevi, L.O., Rasmussen, U., and Bergman, B. (2010). Transfer of a cyanobacterial neurotoxin within a temperate aquatic ecosystem suggests pathways for human exposure. Proc. Natl. Acad. Sci. U. S. A. *107*, 9252–9257. https://doi.org/10.1073/pnas.0914417107.

Joshi, A., and Mueller, L.D. (1993). Directional and stabilizing density-dependent natural selection for pupation height in Drosophila melanogaster. Evolution *47*, 176–184. https://doi.org/10.2307/2410127.

Kain, J., Stokes, C., Gaudry, Q., Song, X., Foley, J., Wilson, R., and de Bivort, B. (2013). Leg-tracking and automated behavioural classification in Drosophila. Nat. Commun. *4*, 1910. https://doi.org/10.1038/ncomms2908.

Khatun, S., Mandi, M., Rajak, P., and Roy, S. (2018). Interplay of ROS and behavioral pattern in fluoride exposed Drosophila melanogaster. Chemosphere *209*, 220–231. https://doi.org/10.1016/j.chemosphere.2018.06.074.

Kurland, L.T. (1988). Amyotrophic lateral sclerosis and Parkinson's disease complex on Guam linked to an environmental neurotoxin. Trends Neurosci. *11*, 51–54. https://doi.org/10.1016/0166-2236(88)90163-4.

Lage, S., Costa, P.R., Moita, T., Eriksson, J., Rasmussen, U., and Rydberg, S.J. (2014). BMAA in shellfish from two Portuguese transitional water bodies suggests the marine dinoflagellate Gymnodinium catenatum as a potential BMAA source. Aquatic toxicology (Amsterdam, Netherlands) *152*, 131–138. https://doi.org/10.1016/j.aquatox.2014.03.029.

Lai, S.L., and Lee, T. (2006). Genetic mosaic with dual binary transcriptional systems in Drosophila. Nat. Neurosci. *9*, 703–709. https://doi.org/10.1038/nn1681.

Lehman, W., Galińska-Rakoczy, A., Hatch, V., Tobacman, L.S., and Craig, R. (2009). Structural basis for the activation of muscle contraction by troponin and tropomyosin. J. Mol. Biol. *388*, 673–681. https://doi.org/10.1016/j.jmb.2009.03.060.

Lobner, D., Piana, P.M., Salous, A.K., and Peoples, R.W. (2007). Beta-N-methylamino-L-alanine enhances neurotoxicity through multiple mechanisms. Neurobiol. Dis. *25*, 360–366. https://doi.org/10.1016/j.nbd.2006.10.002.

Makris, S.L., Raffaele, K., Allen, S., Bowers, W.J., Hass, U., Alleva, E., Calamandrei, G., Sheets, L., Amcoff, P., Delrue, N., and Crofton, K.M. (2009). A retrospective performance assessment of the developmental neurotoxicity study in support of OECD test guideline 426. Environmental health perspectives *117*, 17–25. https://doi.org/10.1289/ehp.11447.

Markow, T.A., Beall, S., and Matzkin, L.M. (2009). Egg size, embryonic development time and ovoviviparity in Drosophila species. J. Evol. Biol. *22*, 430–434. https://doi.org/10.1111/j.1420-9101.2008.01649.x.

Mathis, A., Mamidanna, P., Cury, K.M., Abe, T., Murthy, V.N., Mathis, M.W., and Bethge, M. (2018). DeepLabCut: markerless pose estimation of user-defined body parts with deep learning. Nat. Neurosci. *21*, 1281–1289. https://doi.org/10.1038/s41593-018-0209-y.

Mendes, C.S., Bartos, I., Akay, T., Marka, S., and Mann, R.S. (2013). Quantification of gait parameters in freely walking wild type and sensory deprived Drosophila melanogaster. Elife *2*, e00231. https://doi.org/10.7554/eLife.00231.

Mendes, C.S., Rajendren, S.V., Bartos, I., Marka, S., and Mann, R.S. (2014). Kinematic responses to changes in walking orientation and gravitational load in Drosophila melanogaster. PLoS One *9*, e109204. https://doi.org/10.1371/journal.pone.0109204.

Muñoz-Sáez, E., de Munck García, E., Arahuetes Portero, R.M., Martínez, A., Solas Alados, M.T., and Miguel, B.G. (2015). Analysis of β-N-methylamino-L-alanine (L-BMAA) neurotoxicity in rat cerebellum. Neurotoxicology *48*, 192–205. https://doi.org/10.1016/j.neuro.2015.04.001.

Murch, S.J., Cox, P.A., Banack, S.A., Steele, J.C., and Sacks, O.W. (2004). Occurrence of beta-methylamino-l-alanine (BMAA) in ALS/PDC patients from Guam. Acta Neurol. Scand. *110*, 267–269. https://doi.org/10.1111/j.1600-0404.2004.00320.x.

Narasimha, S., Kolly, S., Sokolowski, M.B., Kawecki, T.J., and Vijendravarma, R.K. (2015). Prepupal building behavior in Drosophila melanogaster and its evolution under resource and time constraints. PLoS One *10*, e0117280. https://doi.org/10.1371/journal.pone.0117280.

Nazir, A., Mukhopadhyay, I., Saxena, D.K., and Chowdhuri, D.K. (2003). Evaluation of the No observed adverse effect level of solvent dimethyl sulfoxide in Drosophila melanogaster. Toxicol. Mech. Methods *13*, 147–152. https://doi.org/10.1080/15376510309846.

Nazir, A., Mukhopadhyay, I., Saxena, D.K., and Kar Chowdhuri, D. (2001). Chlorpyrifos-induced hsp70 expression and effect on reproductive performance in transgenic Drosophila melanogaster (hsp70-lacZ) Bg9. Arch. Environ. Contam. Toxicol. *41*, 443–449. https://doi.org/10.1007/s002440010270.

OECD (2007). Test No. 426: Developmental Neurotoxicity Study. https://doi.org/10.1787/9789264067394-en.

Okamoto, S., Esumi, S., Hamaguchi-Hamada, K., and Hamada, S. (2018). β-N-methylamino-L-alanine (BMAA) suppresses cell cycle progression of non-neuronal cells. Sci. Rep. *8*, 17995. https://doi.org/10.1038/s41598-018-36418-9.

Pablo, J., Banack, S.A., Cox, P.A., Johnson, T.E., Papapetropoulos, S., Bradley, W.G., Buck, A., and Mash, D.C. (2009). Cyanobacterial neurotoxin BMAA in ALS and Alzheimer's disease. Acta Neurol. Scand. *120*, 216–225. https://doi.org/10.1111/j.1600-0404.2008.01150.x.

Pereira, T.D., Aldarondo, D.E., Willmore, L., Kislin, M., Wang, S.S., Murthy, M., and Shaevitz, J.W. (2019). Fast animal pose estimation using deep neural networks. Nat. Methods *16*, 117–125. https://doi.org/10.1038/s41592-018-0234-5.

Peterson, R.T., Nass, R., Boyd, W.A., Freedman, J.H., Dong, K., and Narahashi, T. (2008). Use of non-mammalian alternative models for neurotoxicological study. Neurotoxicology *29*, 546–555. https://doi.org/10.1016/j.neuro.2008.04.006.

Postma, E., van den Herik, H., and van der Maaten, L. (2009). Dimensionality reduction: a comparative review. J. Mach. Learn. Res. *10*, 66–71.

Powsner, L. (1935). The effects of temperature on the durations of the developmental stages of Drosophila melanogaster. Physiol. Zool. *8*, 474–520.

Proctor, E.A., Mowrey, D.D., and Dokholyan, N.V. (2019). β-Methylamino-L-alanine substitution of serine in SOD1 suggests a direct role in ALS etiology. PLoS Comput. Biol. *15*, e1007225. https://doi.org/10.1371/journal.pcbi.1007225.

Ramdya, P., Thandiackal, R., Cherney, R., Asselborn, T., Benton, R., Ijspeert, A.J., and Floreano, D. (2017). Climbing favours the tripod gait over alternative faster insect gaits. Nat. Commun. *8*, 14494. https://doi.org/10.1038/ncomms14494.

Rand, M.D. (2010). Drosophotoxicology: the growing potential for Drosophila in neurotoxicology. Neurotoxicol. Teratol. *32*, 74–83. https://doi.org/10.1016/j.ntt.2009.06.004.

Rand, M.D., Montgomery, S.L., Prince, L., and Vorojeikina, D. (2014). Developmental toxicity assays using the drosophila, Model. Current Protocols in Toxicology *59*. https://doi.org/10.1002/0471140856.tx0112s59.

Rand, M.D., Vorojeikina, D., Peppriell, A., Gunderson, J., and Prince, L.M. (2019). Drosophotoxicology: elucidating kinetic and dynamic pathways of methylmercury toxicity in a Drosophila model. Front. Genet. *10*, 666. https://doi.org/10.3389/fgene.2019.00666.

Rauh, V., Arunajadai, S., Horton, M., Perera, F., Hoepner, L., Barr, D.B., and Whyatt, R. (2011). Seven-year neurodevelopmental scores and prenatal exposure to chlorpyrifos, a common agricultural pesticide. Environmental health perspectives *119*, 1196–1201. https://doi.org/10.1289/ehp.1003160.

Rauh, V.A., Garcia, W.E., Whyatt, R.M., Horton, M.K., Barr, D.B., and Louis, E.D. (2015). Prenatal exposure to the organophosphate pesticide chlorpyrifos and childhood tremor. Neurotoxicology *51*, 80–86. https://doi.org/10.1016/j.neuro.2015.09.004.

Rauh, V.A., Perera, F.P., Horton, M.K., Whyatt, R.M., Bansal, R., Hao, X., Liu, J., Barr, D.B., Slotkin, T.A., and Peterson, B.S. (2012). Brain anomalies in children exposed prenatally to a common organophosphate pesticide. Proc. Natl. Acad. Sci. U. S. A. *109*, 7871–7876. https://doi.org/10.1073/pnas.1203396109.

Rodier, P.M. (1995). Developing brain as a target of toxicity. Environmental health perspectives *103* (*Suppl 6*), 73–76. https://doi.org/10.1289/ehp.95103s673.

Roy-Lachapelle, A., Solliec, M., Bouchard, M.F., and Sauvé, S. (2017). Detection of cyanotoxins in algae dietary supplements. Toxins *9*. https://doi.org/10.3390/toxins9030076.

Sachana, M., Shafer, T.J., and Terron, A. (2021). Toward a better testing paradigm for developmental neurotoxicity: OECD efforts and regulatory considerations. Biology *10*. https://doi.org/10.3390/biology10020086.

Santos, N.C., Figueira-Coelho, J., Martins-Silva, J., and Saldanha, C. (2003). Multidisciplinary utilization of dimethyl sulfoxide: pharmacological, cellular, and molecular aspects. Biochem. Pharmacol. *65*, 1035–1041. https://doi.org/10.1016/s0006-2952(03)00002-9.

Schachat, F.H., Canine, A.C., Briggs, M.M., and Reedy, M.C. (1985). The presence of two skeletal muscle alpha-actinins correlates with troponin-tropomyosin expression and Z-line width. JCB (J. Cell Biol.) *101*, 1001–1008. https://doi.org/10.1083/jcb.101.3.1001.

Schindelin, J., Arganda-Carreras, I., Frise, E., Kaynig, V., Longair, M., Pietzsch, T., Preibisch, S., Rueden, C., Saalfeld, S., Schmid, B., et al. (2012). Fiji: an open-source platform for biological-image analysis. Nat. Methods *9*, 676–682. https://doi.org/10.1038/nmeth.2019.

Schretter, C.E., Vielmetter, J., Bartos, I., Marka, Z., Marka, S., Argade, S., and Mazmanian, S.K. (2018). A gut microbial factor modulates locomotor behaviour in Drosophila. Nature *563*, 402–406. https://doi.org/10.1038/s41586-018-0634-9.

Silva, M.H. (2020). Effects of low-dose chlorpyrifos on neurobehavior and potential mechanisms: a review of studies in rodents, zebrafish, and Caenorhabditis elegans. Birth defects research *112*, 445–479. https://doi.org/10.1002/bdr2.1661.

Skarlatou, S., Hérent, C., Toscano, E., Mendes, C.S., Bouvier, J., and Zampieri, N. (2020). Afadin signaling at the spinal neuroepithelium regulates

central canal formation and gait selection. Cell Rep. *31*, 107741. https://doi.org/10.1016/j.celrep.2020.107741.

Smirnova, L., Hogberg, H.T., Leist, M., and Hartung, T. (2014). Developmental neurotoxicity - challenges in the 21st century and in vitro opportunities. ALTEX *31*, 129–156. https://doi.org/10.14573/altex.1403271.

Sokolowski, M.B., and Bauer, S.J. (1989). Genetic analyses of pupation distance in Drosophila melanogaster. Heredity *62*, 177–183. https://doi.org/10.1038/hdy.1989.26.

Soler, C., Daczewska, M., Da Ponte, J.P., Dastugue, B., and Jagla, K. (2004). Coordinated development of muscles and tendons of the Drosophila leg. Development *131*, 6041–6051.

Sood, K., Kaur, J., Singh, H., Kumar Arya, S., and Khatri, M. (2019). Comparative toxicity evaluation of graphene oxide (GO) and zinc oxide (ZnO) nanoparticles on Drosophila melanogaster. Toxicol. Rep. *6*, 768–781.

Spencer, P.S., Nunn, P.B., Hugon, J., Ludolph, A.C., Ross, S.M., Roy, D.N., and Robertson, R.C. (1987). Guam amyotrophic lateral sclerosis-parkinsonism-dementia linked to a plant excitant neurotoxin. Science *237*, 517–522. https://doi.org/10.1126/science.3603037.

Strauss, R., and Heisenberg, M. (1990). Coordination of legs during straight walking and turning in Drosophila melanogaster. J Comp Physiol [A] *167*, 403–412.

Szczecinski, N.S., Bockemühl, T., Chockley, A.S., and Büschges, A. (2018). Static stability predicts the continuum of interleg coordination patterns in Drosophila. J. Exp. Biol. *221*. https://doi.org/10.1242/jeb.189142.

Tatum-Gibbs, K.R., McKee, J.M., Higuchi, M., and Bushnell, P.J. (2015). Effects of toluene, acrolein and vinyl chloride on motor activity of Drosophila melanogaster. Neurotoxicol. Teratol. *47*, 114–124. https://doi.org/10.1016/j.ntt.2014.11.008.

Tyle, H., Larsen, H., Andersen, L., and Brandt-Lassen, R. (2003). European Union Risk Assessment Report: Toluene (Office for Official Publications of the European Communities).

U.S. EPA (U.S. Environmental Protection Agency). (1998). Health Effects Guidelines OPPTS 870.6300 Developmental Neurotoxicity Study. EPA 712–C–98–239.Available at: http://www.epa.gov/opptsfrs/publications/OPPTS_Harmonized/870_Health_Effects_Test_Guidelines/Series/870-6300.pdf

Uhlmann, V., Ramdya, P., Delgado-Gonzalo, R., Benton, R., and Unser, M. (2017). FlyLimbTracker: an active contour based approach for leg segment tracking in unmarked, freely behaving Drosophila. PLoS One *12*, e0173433. https://doi.org/10.1371/journal.pone.0173433.

Uysal, H., Kızılet, H., Ayar, A., and Taheri, A. (2015). The use of endemic Iranian plant, Echium amoenum, against the ethyl methanesulfonate and the recovery of mutagenic effects. Toxicol. Ind. Health *31*, 44–51. https://doi.org/10.1177/0748233712468019.

Venkatasubramanian, L., Guo, Z., Xu, S., Tan, L., Xiao, Q., Nagarkar-Jaiswal, S., and Mann, R.S. (2019). Stereotyped terminal axon branching of leg motor neurons mediated by IgSF proteins DIP-α and Dpr10. Elife *8*, e42692. https://doi.org/10.7554/eLife.42692.

Wang, S., Wang, S., Lin, J., and Lin, J. (1990). Striated muscle tropomyosin-enriched microfilaments of developing muscles of chicken embryos. J. Muscle Res. Cell Motil. *11*, 191–202. https://doi.org/10.1007/BF01843573.

Wang, Z., Walker, G.W., Muir, D.C.G., and Nagatani-Yoshida, K. (2020). Toward a global understanding of chemical pollution: a first comprehensive analysis of national and regional chemical inventories. Environmental science & technology *54*, 2575–2584. https://doi.org/10.1021/acs.est.9b06379.

Weiss, J.H., and Choi, D.W. (1988). Beta-N-methylamino-L-alanine neurotoxicity: requirement for bicarbonate as a cofactor. Science *241*, 973–975. https://doi.org/10.1126/science.3136549.

Weiss, J.H., Koh, J.Y., and Choi, D.W. (1989). Neurotoxicity of beta-N-methylamino-L-alanine (BMAA) and beta-N-oxalylamino-L-alanine (BOAA) on cultured cortical neurons. Brain Res. *497*, 64–71. https://doi.org/10.1016/0006-8993(89)90970-0.

Wosnitza, A., Bockemuhl, T., Dubbert, M., Scholz, H., and Buschges, A. (2013). Inter-leg coordination in the control of walking speed in Drosophila. J. Exp. Biol. *216*, 480–491. Epub 072012 Oct 078134. https://doi.org/10.1242/jeb.078139.

Wu, S., Tan, K.J., Govindarajan, L.N., Stewart, J.C., Gu, L., Ho, J.W.H., Katarya, M., Wong, B.H., Tan, E.K., Li, D., et al. (2019). Fully automated leg tracking of Drosophila neurodegeneration models reveals distinct conserved movement signatures. PLoS Biol. *17*, e3000346. https://doi.org/10.1371/journal.pbio.3000346.

Xie, J., Wettschurack, K., and Yuan, C. (2020). Review: in vitro cell platform for understanding developmental toxicity. Front. Genet. *11*. https://doi.org/10.3389/fgene.2020.623117.

Zeng, F., Yang, H., Zhou, H.-D., and Wang, Y.-J. (2014). Toluene-induced leukoencephalopathy with characteristic magnetic resonance imaging findings. Neuroimmunol. Neuroinflammation *1*, 92–94. https://doi.org/10.4103/2347-8659.139721.

Zhang, J., Schulze, K.L., Hiesinger, P.R., Suyama, K., Wang, S., Fish, M., Acar, M., Hoskins, R.A., Bellen, H.J., and Scott, M.P. (2007). Thirty-one flavors of Drosophila rab proteins. Genetics *176*, 1307–1322.

Zhou, X., Escala, W., Papapetropoulos, S., Bradley, W.G., and Zhai, R.G. (2009). BMAA neurotoxicity in Drosophila. Amyotroph Lateral Scler. *10*, 61–66. https://doi.org/10.3109/17482960903273445.

Zhou, X., Escala, W., Papapetropoulos, S., and Zhai, R.G. (2010a). β-N-Methylamino-L-Alanine induces neurological deficits and shortened life span in Drosophila. Toxins *2*, 2663–2679. https://doi.org/10.3390/toxins2112663.

Zhou, X., Escala, W., Papapetropoulos, S., and Zhai, R.G. (2010b). β-N-methylamino-L-alanine induces neurological deficits and shortened life span in Drosophila. Toxins *2*, 2663–2679. https://doi.org/10.3390/toxins2112663.

STAR★METHODS

KEY RESOURCES TABLE

REAGENT or RESOURCE	SOURCE	IDENTIFIER
Experimental models: Organisms/strains		
Canton-S	BDSC	RRID:BDSC_64349
Tm1[CC00578]	BDSC	RRID:BDSC_51537
[R22A08]-LexA	BDSC	RRID:BDSC_54692
lexOp-Rab3:YFP	This paper	
Software and algorithms		
FlyWalker	(Mendes et al., 2013)	https://doi.org/10.7554/eLife.00231
Fiji	(Schindelin et al., 2012)	https://fiji.sc
MATLAB 2020	Mathworks	https://www.mathworks.com/products/matlab.html
Imaris 9.5	Oxford instruments	https://imaris.oxinst.com/
RStudio 1.1.442	RStudio	https://www.rstudio.com
GraphPad Prism v6	GraphPad	https://www.graphpad.com/scientificsoftware/prism
Python 3.6.4 Anaconda	Anaconda	https://www.anaconda.com/distribution/
Data processing- Residuals Analysis	This paper	https://github.com/NeurogeneLocomotion/Data-Processing—Residuals-Analysis.git
Data Visualization- Outlier removal and Heatmap	This paper	https://github.com/NeurogeneLocomotion/Data-Visualization–Outlier-removal-and-Heatmap.git
Data visualization- Principal Component Analysis	This paper	https://github.com/NeurogeneLocomotion/Principal-Component-Analysis.git

Lead contact

Further information and requests for resources and reagents should be directed to and will be fulfilled by the lead contact, César S. Mendes (cesar.mendes@nms.unl.pt).

Materials availability

The fly line generated in this study is available from the lead contact without restrictions.

EXPERIMENTAL MODEL AND SUBJECT DETAILS

The full list of *Drosophila melanogaster* strains used in the paper is described in the key resources table. Flies were fed with standart food and kept under constant temperature (25ºC) and humidity (~70%).

METHOD DETAILS

Generation of transgenic lines

The lexOp-Rab3:YFP strain was generated by excising the Rab3:YFP ORF (a gift from Matthew Scott) using NotI and XbaI restriction enzymes and cloning this fragment into a *LexOp* -MCS (pLOT) plasmid (Lai and Lee, 2006). Transgenic lines were generated by standard P-element-mediated transformation procedures in an *yw* background. Lines were selected based on strength and background expression.

Embryo collection

Ten females and five males of wild type CantonS flies were transferred to a cage with a petri dish containing a layer of apple juice and maintained overnight. Produced eggs were collected and transferred to a 70 μm nylon cell strainer (BD Biosciences) with the help of distilled water and a brush. Embryos were submerged in a 50% (v/v) solution of commercial bleach for a few minutes, in order to dechorionate the eggs to test for fertilization. To identify fertilization and viability, each egg was individually observed with a fluorescence stereoscope (SteREO V8, Zeiss) with an Intermediate LED tube FL S, 38 HE GFP - (EX BP 470/40, BS FT 495, EM BP 525/50). Fertilized eggs were selected based on the presence of developing intestine and

movement, distinguishable from non-fertilized ones, which showed a homogeneous white colouring. The former ones were transferred from the container for further experimentation. Twenty five fertilized eggs were transferred to each test vial, ensuring that the same larva:food ratio is kept and thus ensuring a comparable animal size.

Food preparation

Eggs were exposed to tainted and control food, containing 1 gram of food (approximately 1 ml) in a 2 cm diameter vial. For each condition, stock solutions of test compounds were prepared and 5 μL added to a vial of food, except in the case of DMSO (see below). Food was mixed using a handheld drill with a disposable fork with two tines. To obtain a homogenous layer, the vials were centrifuged at 280 g. Lastly, food was left overnight to allow even spreading of test compound by diffusion. For each condition, 3 vials were prepared.

Control experiments were carried out to evaluate potential neurotoxic effects of the solvent DMSO. Three food concentrations were studied, namely 0.07, 70 and 140 mM. The two highest concentrations were obtained by adding 5 and 10 μL, respectively, of pure DMSO (Merk, Darmstadt, Germany) into the food vial. For 0.07 mM, pure DMSO was diluted 100× in water and 5 μL were added to the food vial. For TOL (Sigma-Aldrich, St. Louis, MO, USA), two stock solutions of 10 and 1 mM were prepared using DMSO as solvent. Five μL of these solutions were mixed with fly food to reach a concentration of 5 and 50 μM. Five μL of purchased TOL were used to generate 47.5 mM in fly food. Regarding CPS (Sigma-Aldrich, St. Louis, MO, USA), a stock solution of 1 M was prepared in DMSO. This solution was further diluted in DMSO to obtain 10, 1 and 0.1 mM, and 5 μL of these solutions were added to fly food vials to generate 50, 5 and 0.5 μM, respectively, leading to a constant DMSO of 70 mM (0.5% v/v) in each of these three dose levels. Glycerol-containing food was prepared by micropipetting 5 μL of glycerol (Alfa Aesar, Ward Hill, Ma, USA) per gram of food, corresponding to approximately 68 mM (0.5% v/v) concentration. The amino acid BMAA (Sigma-Aldrich, St. Louis, MO, USA), was dissolved using water as solvent to obtain a stock solution of 1 M. This solution was further diluted to obtain 1000, 100, 10, 1 and 0.1 mM, and 5 μL of these stock solutions were added to fly food vials to obtain 5000, 500, 50, 5 and 0.5 μM final food concentrations, respectively.

Adult animals were kept on normal, untainted food for the FlyWalker assay and imaging experiments. If necessary, food was changed every week.

Survival and pupal climbing positioning

For each exposure condition, 25 fertilized, and viable eggs were placed in each test vial, performed in triplicate, totalling 75 animals. The positioning of the pupa in the vial wall was measured according to four height-locations: I. pupae located inside the food; II. placed slightly above the food; III. positioned up to 1 centimetre (cm) from the food; and IV. occupying the area above 1 cm (Figure 1D). The number of animals reaching pupal stages and eclosing (exiting their pupal cases) were additionally recorded.

Climbing assay

Climbing (or negative geotaxis) assay was carried in 1-week post-eclosion females as previously described (Dinter et al., 2016; Zhou et al., 2009, 2010b). Groups of 10 animals were transferred to 2.5 cm diameter glass vials and after a 30-min period of acclimatization, each tube was gently tapped to the bottom and the number of flies crossing a line at 8 cm height within a period of 10 s was scored. 3 consecutive readings were carried out per group. For each condition 50 flies were analysed.

Kinematic analysis

Kinematic behavioural experiments were carried out as described previously (Mendes et al., 2013). After eclosion, flies were collected and kept for 3 days in a new vial containing normal fly food and a humid paper filter to prevent contamination of the walking arena. Individual flies were placed into a walking chamber and filmed with a Photron (Tokyo, Japan) Mini UX-100 camera using a Nikon (Tokyo, Japan) AF 24-85mm lens at 250 frames per second (fps). For each condition, 10 animals were filmed twice, generating 20 videos. Kinetic parameters of fly movement were obtained through analyses of obtained videos, using the FlyWalker software package (Mendes et al., 2013). All parameters were normalized to body length.

In addition to the previously published kinematic parameters (Mendes et al., 2013, 2014), two additional parameters were quantified:

- **Stance Straightness:** Ratio between the distance from AEP to PEP (stance phase) and the path described by the tarsal contacts relative to the body (stance trace).
- **Body displacement ratio:** Ratio between of the distance traveled over the body path.

Leg dissection and microscopy

T1 legs were isolated using a dissecting microscope from selected animals with the correct genotype. Legs were kept in cold PBS, followed by a quick rinse with ethanol to remove the wax from the cuticle, preventing floating and maintaining legs submerged during the procedure. After three washes in PBS, legs were fixed overnight in 4% paraformaldehyde in PBS at 4°C. After three washes in PBS, legs were mounted on glass slides in glycerol and imaged with a Zeiss (Oberkochen, Germany) LSM710 confocal microscope with a 40× objective using a 514 nm excitation laser and a emission windows of 519-582 nm (for YFP), and a 594 nm excitation laser and a emission windows of 599-797nm (for auto-fluorescence).

QUANTIFICATION AND STATISTICAL ANALYSIS

FlyWalker data

Kinematic parameters were extracted using the FlyWalker Software, in which each video resulted a single data point (Mendes et al., 2013). Since many of the measured gait parameters vary with speed, we analyzed the data for these parameters by firstly determining the best-fit regression model for the control experiment. Subsequently the residual values for each experimental group in relation to this regression model were determined, using RStudio 1.1.442 (Mendes et al., 2014). The residual dataset was subsequently tested for normality and homoscedasticity using the Shapiro-Wilk and Levene Tests. Statistical significance between the control and each of the experimental groups were determined using Kruskal-Wallis analysis of variance followed by Dunn's post hoc test (for non-normal distributions) or one-way-ANOVA followed by Tukey's post hoc test (for normal distributions). Significant differences were represented by a Heatmap where each column represents the different groups compared with the control and in each line the kinematic parameters. Red and blue bars indicate an increased and decreased value, respectively. Lighter, intermediate, and darker colors indicate a p value of <0.05, <0.01 and <0.001, respectively.

PCA

To have a more succinct representation of the data we used Principal Component Analysis (PCA), an unsupervised dimensionality reduction method. PCA finds a linear projection of the data from a high-dimensional space onto a lower-dimensional subspace, while maximizing variance of the projected data, and thus retains meaningful information, resulting in a description of the data as a function of a smaller set of uncorrelated variables (or principal components). The data was first pre-processed by centering and scaling, after which the PCA algorithm computed the covariance matrix in order to determine the correlation between variables and calculated the eigenvectors and eigenvalues of the covariance matrix in order to identify the principal components. We chose the first three principal components to visualize the data. The first two components were chosen to generate a two-dimensional plot. Each dot in the plots corresponds to a video, representing these new abstract variables. Color-coded dots were used to distinguish specific groups. As such, clusters of dots reflect similar walking patterns, shared by the corresponding flies.

Microscopy data

TropGFP images were analyzed using Fiji for profile tracing (Schindelin et al., 2012), and a MATLAB (MathWorks Inc, Natick, MA, EUA) custom script for peak signal measurement and coefficient of variation calculation. Muscle profiles were obtained using a Fiji line tool manually placed along each muscle fibre in locations with good signal in different locations from 4 independent images for each condition. Muscle profiles were then analysed using a custom MATLAB script, which detected each peak ("find-peaks" function) and quantified the periodicity of each profile. The coefficient of variation (standardized measure of dispersion of a probability distribution) of each profile was then calculated and plotted.

Motor neuron imaging data was analysed using a custom MATLAB script. Leg upper and lower boundaries were segmented using the cuticle autofluorescence signal. Noise was reduced using a gaussian filter

function (imgaussfilt) with sigma 2 and a global threshold was determined. With these two boundaries a central leg axis was detected and used for subsequent calculation. The neuronal profile was binarized using an OTSU global threshold and the intensity centre of mass in each position was found along the proximal-distal axis.

For the ratio between NMJ penetration depth (starting from the trochanter-femur joint) and the total length of the longest branch (starting from the trochanter-femur joint) images were processed in Imaris 9.5 (Oxford instruments, Abingdon, U.K.) using the filament tracer tool semi-automatically (results were manually curated) and measurements were made using the measurement and statistics tools.

All other measurements were carried out using the Imaris 9.5 imaging analysis package.

Graphs and statistical analyses

Bar graphs represent the average percentage of animals surviving each developmental stage ± SEM. Box-plots represent the median as the middle line, with the lower and upper edges of the boxes representing the 25 and 75% quartiles, respectively; the whiskers represent the range of the full dataset, excluding outliers (open circles). Outliers are defined as any value that is 1.5 times the interquartile range below or above the 25 and 75% quartiles, respectively. Climbing assay results were tested using one-way-ANOVA followed by Tukey's post hoc test (Figure 3D). For microscopy experiments (Figures 7 and S10), plots represent the mean as the middle line ± SD. Statistical analysis with one-way ANOVA followed by Tukey's post hoc test (for normal distributions) or Kruskal-Wallis followed by Dunn's post hoc test (for nonnormal distribution). Statistical analysis was performed using custom MATLAB and Python scripts and GraphPad Prism. *$p < 0.05$; **$p < 0.01$; ***$p < 0.001$; ****$p < 0.0001$; n.s., not significant.